Supplementary Information

New High Performance Digital Memory Devices Fabricated with DNA and DNA-Mimics

Jinseok Lee, Yongjin Kim, Changsub Kim and Moonhor Ree*

Department of Chemistry, Division of Advanced Materials Science, Polymer Research Institute, and Pohang Accelerator Laboratory, Pohang University of Science and Technology, Pohang 37673, Republic of Korea

Experimental Section

Materials

StDNA (1.3×10^6 molecular weight) and CtDNA (1.62×10^6 molecular weight) were purchased in a sodium salt form from Sigma-Aldrich Chemical Company (St. Louis, MO, USA). 2,2'-Azobis(iso butyronitrile) (AIBN) was obtained from Acros Organics Company (Seoul, Korea) and recrystallized twice from ethanol and then dried under vacuum prior to use. *N*-(3-Dimethylaminopropyl)-*N*′-ethylcarbodiimide hydrogenchloride (EDC) was purchased from Tokyo Chemical Industry Company (Tokyo, Japan) and used as received. Other chemical compounds including 4-hydroxybutyl acrylate were received from Sigma-Aldrich Chemical Company (St. Louis, MO, USA) and used without further purifications.

Natural DNAs

The DNA salts were further treated in two different ways. Firstly, the DNA salts were converted to a natural form as follows. Each DNA salt was dissolved in distilled, sterilized water as a concentration of 0.01 g/mL. The DNA salt solution (10 mL) was mixed with a 4 M sodium chloride

solution (0.53 mL) and 70 % ethanol (27 mL) at ca. 20 °C. Then, DNA was precipitated from the mixture solution by centrifugation at 12000 rpm for 10 min. The obtained DNA pellets were washed with 70% ethanol twice and then dried at room temperature in ambient condition. Secondly, the DNA sodium salts were converted to their surfactant complex (StDNA-surfactant and CtDNA-surfactant). Each DNA salt was dissolved in distilled water, giving a solution with 2.0 mg/mL concentration. Cetyltrimethylammonium bromide (CTAB), a surfactant, was dissolved in distilled water at 30 °C as a concentration of 7.3 mg/mL. The CTAB solution (10 mL) was overly added into each DNA salt solution (20 mL) at 30 °C under stirring and then the mixture was stirred for additional 1 h at the temperature, giving DNA-surfactant complex precipitates. The precipitates were collected by filtration, washed with distilled water at 30 °C, and dried in vacuum at room temperature for 2 days.

Synthesis of DNA-Mimicking Brush Polymers

Two series of brush polymers containing nucleobases were newly synthesized in a two-step manner as DNA mimicking polymers, as shown Scheme 1. In the first step, a P4HBA was synthesized as a base polymer from 4-hydroxybutyl acrylate via reversible addition-fragmentation chain transfer (RAFT) polymerization. In similar manner, a P9HNA was synthesized for the second series of DNA mimicking polymers. In the second step, each nucleobase derivative having a carboxylic acid group was incorporated into the hydroxyl groups of P4HBA or P9HNA via esterification reaction. As a result, a series of DNA mimicking brush polymers based on P4HBA was obtained; another series of DNA mimicking brush polymers based on P9HNA was obtained. The synthesis details of these brush polymers were given below.

Polymerizations. Poly(4-hydroxybutyl acrylate) (P4HBA) was synthesized via reversible addition-fragmentation chain transfer (RAFT) polymerization. A Schlenk tube was charged with monomers, 4-hydroxybutyl acrylate (1 g, 6.93 mmol) in anhydrous DMF (3.5 mL, 2 M solution), AIBN (5.69 mg, 34.7 μmol) and of 3-benzylsulfanylthiocarbonylsulfanylpropionic acid, a chain transfer agent (CTA) (18.8 mg, 69.4 μmol). The reaction mixture was degassed by three freeze-

pump-thaw cycles and then stirred at 60 °C for 24 h. After the reaction mixture was cooled to room temperature, the polymer was purified by repeated precipitation from diethyl ether solution. The precipitate was then collected by vacuum filtration and dried, giving the target P4HBA product. Yield = 99 %. The obtained polymer product was characterized by using a nuclear magnetic resonance (NMR) spectrometer (model AV300 FT-NMR, Bruker, Rheinstetten, BW, Germany) with proton (^{1}H) and carbon (^{13}C) probes; dimethylsulfoxide (DMSO-d_6) was used as a solvent and tetramethylsilane was used as an internal standard. The product was also identified by using an infrared (IR) spectrometer (model Model Research Series 2, ATI Mattson, Madison, WN, USA) equipped with a liquid nitrogen-cooled mercury cadmium telluride (MCT) detector. ^{1}H NMR (300 MHz, DMSO-d_6, δ (ppm)): 7.24 (t, 5H, aromatic protons from CTA), 4.44-4.41 (m, 100H), 4.12-3.87 (m, 200H), 3.42-3.37 (m, 200H), 2.36-1.64 (br, 300H), 1.63-1.21 (m, 400H) (Fig. S21); ^{13}C NMR (75 MHz, DMSO-d_6, δ (ppm)): 24.7, 28.6, 40.9, 48.5, 60.1, 64.1, 173.9 (Fig. S22a); IR (film, ν (cm^{-1})): 3371, 2952, 1729, 1646, 1534, 1451, 1251, 1168, 1044 (Fig. S23a).

From the ^{1}H NMR spectroscopy analysis result, the number-average degrees of polymerization (DP_{nmr}) of the P4HBA product was determined to be 99. Therefore, the number-average molecular weight ($M_{n,nmr}$) was calculated to 14500 from the DP_{nmr} value and the molar mass of the repeat unit.

In similar manner, poly(9-hydroxynonyl acrylate) (P9HNA) was synthesized from 9-hydroxynonyl acrylate (9-HNA). Yield: 97 %. ^{1}H NMR (300 MHz, DMSO-d_6, δ (ppm)): 7.24 (t, 5H, aromatic protons from CTA), 4.44-4.41 (m, 100H), 4.12-3.87 (m, 200H), 3.42-3.37 (m, 200H), 2.36-1.64 (br, 300H), 1.63-1.21 (m, 1400H) (Fig. S24); IR (film, ν (cm^{-1})): 3437, 2931, 2856, 1731, 1666, 1458, 1397, 1256, 1166, 1056 (Fig. S25a). From the NMR spectroscopy analysis, the P9HNA product was determined to have DP_{nmr} = 95 and $M_{n,nmr}$ = 20700.

9-Hydroxynonyl acrylate (9-HNA). The synthesis of 9-hydroxynonyl acrylate (9-HNA), 1,9-nonanediol (4.365 g, 27.2 mmol), triethyl amine (TEA) (3.791 mL, 27.2 mmol), and hydroquinone were added to 80 mL THF, and the mixture was cooled to 0 °C. Acryloyl chloride (2 mL, 24.5 mmol) was slowly added. Thereafter, the solution was stirred at 0 °C for 4 h and continuously stirred at room temperature for 12 h. Then the reaction mixture was extracted with ethyl acetate. The organic layer was separated, washed twice with water (150 mL), and dried with $MgSO_4$. After the solvent was evaporated off, the residue was purified by column chromatography with a 1:1

mixture of *n*-hexane and ethyl acetate giving the product 9-hydroxynonyl acrylate in white powder. Yield = 79 %. ^{1}H NMR (300 MHz, $CDCl_3$, δ (ppm)): 6.35-6.41 (d, 1H), 6.10-6.20 (q, 1H), 5.74-5.78 (d, 1H), 4.10-4.18 (t, 2H), 3.61-3.65 (t, 2H), 1.62-1.66 (br, 4H), 1.26 (s, 10H) (Fig. S24).

Chain transfer agent (CTA). The synthesis of 3-benzylsulfanylthiocarbonylsulfanylpropionic acid, a chain transfer agent (CTA) was carried out according to the procedure reported in the literature.[S1] 3-Mercaptopropionic acid (2 mL, 23 mmol) was slowly added to an aqueous solution of potassium hydroxide (2.6 g, 48 mmol KOH in 25 mL water). After the dropwise addition of carbon disulfide (3 mL, 31 mmol), the orange solution was stirred overnight. After the addition of benzyl bromide (3.96 g, 23 mmol), the reaction mixture was heated at reflux for 12 h. After cooling and the addition of chloroform (30 mL), the reaction mixture was acidified with HCl until the organic layer was yellow. The water phase was extracted twice with 20 mL chloroform. The combined organic layer was washed with brine and dried over sodium sulfate. After the solvent was evaporated off, the residue was purified by column chromatography with a 3:1 mixture of *n*-hexane and ethyl acetate giving the target product CTA in yellow powder. Yield = 90 %. ^{1}H NMR (300 MHz, $CDCl_3$, δ (ppm)): 10.1 (s, 1H), 7.39–7.18 (m, 5H), 4.61 (s, 2H), 3.62 (t, 2H), 2.84 (t, 2H).

3-(9-Adeninyl)propionic acid. Adenine (10 g, 74 mmol) and sodium ethoxide (NaOEt, 2.7 g, 37.6 mmol) was suspended in dry ethanol (EtOH, 200 mL). Then, EtOAc was added to suspension. After heating at reflux for 2 h, the used solvent was removed by filtration. Remaining precipitates were recrystallized from EtOH. Ethyl 3-(9-adeninyl)propionate were obtained with 77 % yield. The product was identified in deuterated chloroform ($CDCl_3$) with tetramethylsilane as an internal standard by nuclear magnetic resonance (NMR) spectroscopy analysis with a proton (^{1}H) probe using a Bruker spectrometer (model AV300 FT-NMR, Rheinstetten, BW, Germany). ^{1}H NMR (300 MHz, $CDCl_3$, δ (ppm)): 1.20-1.23 (t, 3 H), 2.91-2.93 (t, 2 H), 4.11-4.16 (q, 2 H), 4.47-4.51 (t, 2 H), 5.49 (s, 2 H), 7.87 (s, 1 H), 8.35 (s, 1 H) (Fig. S26a).

To a one-necked 200-ml round bottom flask equipped with a reflux condenser was added ethyl 3-(9-adeninyl) propionate (2.35 g, 0.01 mol) and 3 *N* hydrochloric acid (75 mL). The solution was heated at reflux for 3 hours and neutralized to pH 10 with sodium hydroxide pellets (8.5 g, 0.21 mol). Addition of concentrated hydrochloric acid resulted in a precipitate forming at pH 6-7. The final pH of the mixture was 3. The acidified mixture was cooled overnight and the resulting solids were collected and dried. Yield = 81 %. The product was identified in deuterated dimethylsulfoxide

(DMSO-d_6) by ^{1}H NMR analysis. ^{1}H NMR (300 MHz, DMSO-d_6, δ (ppm)): 2.40 (t, 2 H), 4.24 (t, 2 H), 7.10 (s, 2 H), 8.04 (s, 1 H), 8.13 (s, 1 H), 12.5 (br, 1 H) (Fig. S26b).

9-(2-Carboxyethyl)guanine. To a solution of 2-amino-6-chloropurine (3.0 g, 17.7 mmol), dissolved in dry methanol (MeOH, 60 mL), sodium methoxide (NaOMe, 22 g, 4.07 mmol) was added and the mixture refluxed for 2 h under nitrogen. *Tert*-butyl acrylate (5.30 g, 41.3 mmol) was added and the mixture refluxed for additional 18 h. The solvent was evaporated and the crude residue dissolved in water. The product was separated as a fine precipitate that was filtered and crystallized from hot water, giving 2-amino-9-(2-*tert*-butoxycarbonylethyl)-6-chloropurine. Yield = 47 %. ^{1}H NMR (300 MHz, DMSO-d_6, δ (ppm)): 1.32 (s, 9 H), 2.83 (t, 2 H), 4.25 (t, 2 H), 6.94 (br, 2 H), 8.10 (s, 1 H) (Fig. S27a).

To a one-necked 200-ml round bottom flask equipped with a reflux condenser was added 2-amino-9-(2-*tert*-butoxycarbonylethyl)-6-chloropurine (2.42 g, 0.01 mol) and 3 *N* hydrochloric acid (75 mL). The solution was heated at reflux for 3 h and then cooled to room temperature, followed by neutralization to pH 10 with sodium hydroxide pellets (8.5 g, 0.21 mol). The addition of concentrated hydrochloric acid resulted in a precipitate forming at pH 6-7. The final pH of the mixture was 3. The acidified mixture was cooled overnight and the resulting solids were collected and dried. Yield = 73 %. ^{1}H NMR (300 MHz, DMSO-d_6, δ (ppm)): 2.77 (t, 2 H), 4.11 (t, 2 H), 6.49 (s, 2 H), 7.64 (s, 1 H), 10.6 (s, 1 H), 12.5 (br, 1 H) (Fig. S27b).

1-Carboxymethyluracil. Uracil (10.1 g, 89.7 mmol), chloroacetic acid (15.1 g, 160 mmol), and potassium hydroxide (22.1 g, 394 mmol) were added to 200 mL water, and the mixture was heated to reflux under stirring. After 1 h, the resulting solution was cooled to 25 °C and acidified to pH 2 with concentrated aqueous HCl. The solution was cooled to 4 °C; after 12 h the product was isolated by vacuum filtration. The product was dried, giving the target product in white crystalline solid. Yield = 68%). ^{1}H NMR (300 MHz, DMSO-d_6, δ (ppm)): 4.41 (s, 2 H), 5.61 (d, 1 H), 7.60 (d, 1 H), 11.4 (s, 1H), 13.2 (s, 1H) (Fig. S28).

N^4-Acetyl-1-carboxymethylcytosine. Cytosine (2.00 g, 18 mmol) and acetic anhydride (3.78 g, 37.0 mmol) were dissolved in pyridine (40 mL) and stirred at room temperature for 24 h. The reaction mixture was precipitated in cold water and filtered. The precipitates were washed with water several times and dry in vacuum. Yield = quantitative. N^4-acetylcytosine was obtained. ^{1}H

NMR (300 MHz, DMSO-d_6, δ (ppm)): 2.06 (s, 3 H), 7.03 (s, 1 H), 7.74 (s, 1 H), 11.1 (br, 2 H) (Fig. S29a).

N^4-acetylcytosine (3 g, 19.6 mmol) was dissolved in 50 mL of dry dimethylformamide (DMF) and 3.07 mL (20.6 mmol) of 1,8-diazabicyclo[5.4.0]undec-7-ene (DBU) was added. After 2 min, 3.5 mL (23.5 mmol) of *tert*-butyl bromoacetate was added dropwise. After stirring for 2 h at room temperature the mixture was concentrated to dryness. The residue was purified by silica gel chromatography and the product was eluted with a 0-5% MeOH gradient in dichloromethane. N^4-acetyl-1-tert-butoxycarbonylmethylcytosine was obtained. Yield = 58 %. ^{1}H NMR (300 MHz, $CDCl_3$, δ (ppm)): 1.47 (s, 9 H) 2.28 (s, 3 H), 4.51 (s, 2 H), 7.48 (d, 1 H), 7.56 (d, 1 H), 10.3 (s, 1H) (Fig. S29b).

N^4-acetyl-1-tert-butoxycarbonylmethylcytosine (2.9 g, mmol) was dissolved in trifluoroacetic acid (TFA, 25 mL) and stirred at room temperature for 40 min. After the reaction, the solution was precipitated in diethyl ether. The precipitates were washed with diethyl ether several times and dried. N^4-acetyl-1-carboxymethylcytosine was obtained. Yield = 88 %. ^{1}H NMR (300 MHz, DMSO-d_6, δ (ppm)): 2.08 (s, 3 H), 4.54 (s, 2 H), 7.19 (d, 1 H), 8.03 (d, 1 H), 10.9 (s, 1H), 13.1 (s, 1H) (Fig. S29c).

Brush polymers containing nucleobase moieties. P4HBA (0.155 g, 1.0 mmol OH) or P9HNA (0.22 g, 1.0 mmol OH), nucleobase derivatives (1.2 mmol), N-(3-dimethylaminopropyl)-N′-ethylcarbodiimide hydrogenchloride (EDC, 0.292 g, 1.44 mmol) and 4-(dimethylamino)-pyridine (DMAP, 0.093 g, 0.72 mmol) were dissolved in DMF (8 mL) and stirred at 45 °C for 24 h. After the reaction was completed, the reaction mixture was precipitated in MeOH and filtered. The residue was dissolved in DMF (5 mL) and insoluble part was filtered. The filtrate was precipitated in MeOH and filtered. To remove excess nucleobase derivatives from the polymer completely, these steps were repeated several times. The obtained products were identified by NMR and IR spectroscopy analyses. The spectroscopy analyses confirmed that the individual esterification reactions were carried out with 100% yield.

P4HBA-A. $M_{n,nmr}$ = 33200. ^{1}H NMR (300 MHz, DMSO-d_6, δ (ppm)): 8.14 (s, 1H), 8.13 (s, 1H), 7.21 (s, 2H), 4.37 (t, 2H), 3.87 (m, 4H), 2.94 (t, 2H), 2.36-1.64 (br, 3H), 1.63-1.21 (m, 4H) (Fig. S30a); ^{13}C NMR (75 MHz, DMSO-d_6, δ (ppm)): 24.7, 28.6, 33.4, 40.3, 60.1, 64.1, 118.6,

140.8, 149.3, 152.3, 155.8, 170.5, 173.8 (Fig. S22b); IR (film, ν (cm^{-1})): 3438, 3324, 3164, 2952, 2864, 1729, 1646, 1599, 1517, 1416, 1475, 1257, 1186, 1050 (Fig. S23b).

P4HBA-G. $M_{n,nmr}$ = 34800. ^{1}H NMR (300 MHz, DMSO-d_6, δ (ppm)): 10.6 (s, 1H), 7.62 (s, 1H), 6.45 (s, 2H), 4.37 (t, 2H), 3.87 (m, 4H), 2.94 (t, 2H), 2.36-1.64 (br, 3H), 1.63-1.21 (m, 4H) (Fig. S30b); ^{13}C NMR (75 MHz, DMSO-d_6, δ (ppm)): 24.4, 28.5, 33.4, 40.9, 60.0, 63.5, 116.2, 137.3, 151.0, 153.4, 156.8, 170.4, 179.0 (Fig. S22c); IR (film, ν (cm^{-1})): 3455, 3335, 3159, 2959, 2733, 1731, 1698, 1634, 1366, 1175 (Fig. S23c).

P4HBA-T. $M_{n,nmr}$ = 30900. ^{1}H NMR (300 MHz, DMSO-d_6, δ (ppm)): 11.4 (s, 1H), 7.47 (s, 1H), 4.45 (s, 2H), 4.07-3.87 (m, 4H), 2.36-1.64 (br, 3H), 1.74 (s, 3H), 1.63-1.21 (m, 4H) (Fig. S30c); ^{13}C NMR (75 MHz, DMSO-d_6, δ (ppm): 11.8, 24.5, 30.2, 40.9, 48.5, 61.6, 64.4, 108.6, 141.4, 150.8, 164.2, 168.2 (Fig. S22d); IR (film, ν (cm^{-1})): 3530, 3214, 3100, 3058, 2964, 2809, 1729, 1688, 1461, 1420, 1389, 1354, 1198 (Fig. S23d).

P4HBA-U. $M_{n,nmr}$ = 29500. ^{1}H NMR (300 MHz, DMSO-d_6, δ (ppm)): 11.4 (s, 1H), 7.61 (s, 1H), 5.58 (s, 1H), 4.49 (s, 2H), 4.07-3.87 (m, 4H), 2.36-1.64 (br, 3H), 1.63-1.21 (m, 4H) (Fig. S30d); ^{13}C NMR (75 MHz, DMSO-d_6, δ (ppm)): 24.5, 25.0, 28.6, 39.9, 48.4, 63.6, 64.6, 101.0, 145.7, 150.9, 163.7, 168.1, 173.9 (Fig. S22e); IR (film, ν (cm^{-1})): 3554, 3220, 3100, 3053, 2958, 1725, 1689, 1461, 1390, 1347, 1199 (Fig. S23e).

P4HBA-C. $M_{n,nmr}$ = 33600. ^{1}H NMR (300 MHz, DMSO-d_6, δ (ppm)): 10.6 (s, 1H), 8.03 (s, 1H), 7.19 (s, 2H), 4.61 (s, 2H), 3.87 (m, 4H), 2.09 (s, 3H), 2.01-1.64 (br, 3H), 1.63-1.21 (m, 4H) (Fig. S30e); ^{13}C NMR (75 MHz, DMSO-d_6, δ (ppm)) : 24.5, 34.4, 40.0, 50.6, 63.5, 64.4, 95.3, 150.4, 155.2, 162.9, 167.8, 171.0, 173.9 (Fig. S22f); IR (film, ν (cm^{-1})): 3450, 3294, 3234, 3144, 3083, 2957, 1731, 1665, 1563, 1491, 1365, 1309, 1449, 1224, 1194, 1082 (Fig. S23f).

P9HNA-A. $M_{n,nmr}$ = 40600. ^{1}H NMR (300 MHz, DMSO-d_6, δ (ppm)): 8.14 (s, 1H), 8.13 (s, 1H), 7.21 (s, 2H), 4.37 (t, 2H), 3.87 (m, 4H), 2.94 (t, 2H), 2.36-1.64 (br, 3H), 1.63-1.21 (m, 14H) (Fig. S31a); IR (film, ν (cm^{-1})): 3269, 3114, 2931, 2856, 1731, 1666, 1604, 1477, 1420, 1363, 1323, 1197, 1082 (Fig. S25b).

P9HNA-G. $M_{n,nmr}$ = 42200. ^{1}H NMR (300 MHz, DMSO-d_6, δ (ppm)): 10.6 (s, 1H), 7.62 (s, 1H), 6.45 (s, 2H), 4.37 (t, 2H), 3.87 (m, 4H), 2.94 (t, 2H), 2.36-1.64 (br, 3H), 1.63-1.21 (m, 14H) (Fig. S31b); IR (film, ν (cm^{-1})): 3339, 2927, 2854, 1760, 1731, 1695, 1681, 1635, 1602, 1558, 1537,

1526, 1513, 1465, 1437, 1420, 1374, 1362, 1173 (Fig. S25c).

P9HNA-T. $M_{n,nmr}$ = 38300. ^{1}H NMR (300 MHz, DMSO-d_6, δ (ppm)): 11.4 (s, 1H), 7.47 (s, 1H), 4.45 (s, 2H), 4.07-3.87 (m, 4H), 2.36-1.64 (br, 3H), 1.74 (s, 3H), 1.63-1.21 (m, 14H) (Fig. S31c); IR (film, ν (cm^{-1})): 3529, 3218, 3065, 2929, 2858, 1730, 1468, 1375, 1206, 1168, 1064 (Fig. S25d).

P9HNA-U. $M_{n,nmr}$ = 36900. ^{1}H ^{1}H NMR (300 MHz, DMSO-d_6, δ (ppm)): 11.4 (s, 1H), 7.61 (s, 1H), 5.58 (s, 1H), 4.49 (s, 2H), 4.07-3.87 (m, 4H), 2.36-1.64 (br, 3H), 1.63-1.21 (m, 14H) (Fig. S31d); IR (film, ν (cm^{-1})): 3553, 3244, 3100, 3061, 2929, 2857, 1729, 1452, 1391, 1353, 1203, 1048 (Fig. S25e).

P9HNA-C. $M_{n,nmr}$ = 41000. ^{1}H NMR (300 MHz, DMSO-d_6, δ (ppm)): 10.6 (s, 1H), 8.03 (s, 1H), 7.19 (s, 2H), 4.61 (s, 2H), 3.87 (m, 4H), 2.09 (s, 3H), 2.01-1.64 (br, 3H), 1.63-1.21 (m, 14H) (Fig. S31e); IR (film, ν (cm^{-1})): 3514, 3296, 3238, 3146, 3084, 2929, 2857, 1735, 1668, 1566, 1494, 1451, 1363, 1310, 1223, 1194, 1107, 1049 (Fig. S25f).

Measurements

The products in the individual synthesis steps were identified in deuterated chloroform ($CDCl_3$) or dimethylsulfoxide (DMSO-d_6) with tetramethylsilane as an internal standard by nuclear magnetic resonance (NMR) spectroscopy analysis with proton (^{1}H) and/or carbon (^{13}C) probe using a Bruker spectrometer (model AV300 FT-NMR, Rheinstetten, BW, Germany). Thermogravimetric analysis (TGA) and differential scanning calorimetry (DSC) measurements were carried out under a nitrogen atmosphere using a thermogravimeter (model TG/DTA 6200, Seiko Instruments, Tokyo, Japan) and a calorimeter (model DSC 6200, Seiko Instruments). A rate of 10.0 °C/min was employed for heating and cooling runs. Infrared (IR) analysis was performed using a spectrometer (model Model Research Series 2, ATI Mattson, Madison, WN, USA) equipped with a liquid nitrogen-cooled mercury cadmium telluride (MCT) detector. Optical properties were measured using an ultraviolet-visible (UV-vis) spectrometer (model S-3100, Scinco, Seoul, Korea). Cyclic voltammetry (CV) was carried out in 0.1 M tetrabutylammonium tetrafluoroborate in acetronitrile using an electrochemical

workstation (IM6ex impedance analyzer, ZAHNER-Elektrik, Kronach, Germany) with a platinum gauze counter electrode and an Ag/AgCl (saturated KCl) reference electrode, and the polymers were coated on the gold (Au) electrode deposited on silicon wafer. A scan rate of 100 mV/s was employed. From the UV-vis spectroscopy and CV data, E_{HOMO} and E_{LUMO} were estimated; details were in Supplementary Information. Atomic force microscopy (AFM) analysis was carried out using a scanning probe microscope (Multimode, Nanoscope Ⅲa, Veeco, Santa Clara, CA, USA) in tapping mode, which was equipped with a J-scanner; noncoated silicon etched probes (model TESP, Veeco). GIXS measurements were conducted at the 3C and 9A beamlines [S2-S4] of PAL. Samples were measured at a sample-to-detector distance (SDD) of 210.11 mm or 223.70 mm. All GIXS measurements were carried out at room temperature. Scattering data were typically collected for 30–60 s using a two-dimensional (2D) charge-coupled detector (CCD) (model Rayonix 2D Mar, Evanston, IL, USA) and an X-ray radiation source with a wavelength (λ) of 0.1180 nm or 0.1110 nm. The incidence angle α_i of X-ray beam was set in the range 0.140–0.180°, which is between the critical angles of the polymer films and the silicon substrate ($\alpha_{c,f}$ and $\alpha_{c,s}$). Scattering angles were corrected according to the positions of the X-ray beams with respect to a precalibrated sucrose and silver behenate (TCI, Tokyo, Japan) powder. Aluminium foil pieces were applied as a semitransparent beam stop, because the intensity of the specular reflection from the substrate is much stronger than the intensity of GIXS near the critical angle. *I–V* measurements were carried out using a Keithley semiconductor analyzer (model 4200-SCS, Keithley, Cleveland, Ohio, USA). All electrical experiments were conducted under ambient condition at room temperature.

Film Preparation and Device Fabrication

For the DNA and brush polymer samples, solutions with a concentration of 0.1 or 1.0 wt% were prepared as follows. The solutions (0.1 wt%) of DNA salts and their natural forms were prepared by dissolving in distilled water and subsequent mixing with tetrahydrofuran (THF) (here, water and THF were in 1:1 volume ratio). For the DNA-surfactant complexes, solutions with 1.0 wt%

concentration were prepared in ethanol. For the brush polymer samples, solutions (1.0 wt%) were prepared. Methanol was used for P4HBA and P9HNA. Dimethyl sulfoxide (DMSO) was used for P4HBA-G, whereas dimethylformamide (DMF) was used for the other brush polymers. Each solution was filtered through polytetrafluoroethylene membrane microfilters with a pore size of 0.22 μm. The obtained individual solutions were spin-coated on precleaned silicon (Si) substrates with and without aluminum (Al) electrode depositions. The coated films of DNA salts and their natural form were dried in vacuum at room temperature for 1 day, whereas the DNA-surfactant films were dried in vacuum at 30 °C for 1 day. The P4HBA and P9HNA films were dried in vacuum at 40 °C for 12 h; all brush polymer films were dried in vacuum at 65 °C for 12 h. Some of the brush polymer films were further annealed at room temperature under vapors of various solvents (THF, $CHCl_3$), toluene, carbon disulfide (CS_2), 1,2-dichloroethane, and methanol). The thicknesses of all obtained films were measured by using a spectroscopic ellipsometer (model M2000, Woollam, Lincoln, NE, USA). For device fabrications, Al bottom electrodes with a thickness of 30 nm were prepared on Si substrates with 300 nm thick oxide layer by electron-beam sputtering through a shadow mask. Al top electrodes with a thickness of 100 nm were deposited onto the polymer films through a shadow mask by thermal evaporation under a pressure of 10^{-6} torr. The obtained cell size was in the range of 100 × 100 to 200 × 200 μm^2.

Determination of E_{HOMO} and E_{LUMO}

The measured UV-vis spectra and CV data are given in Figs. S32-S37. From the UV-vis spectra (Figs. S29-S31), band gaps were determined. From the CV data (Figs. S35-S37), the oxidation half-wave potentials ($E_{1/2}$) versus Ag/AgCl were determined. In addition, the $E_{1/2}$ for the external ferrocene/ferrocenium (F_c/F_c^+) standard was measured to be 0.57 V vs Ag/AgCl in acetonitrile. Assuming that the E_{HOMO} level for the F_c/F_c^+ standard is –4.80 eV with respect to the zero vacuum level, the E_{HOMO} levels of DNAs and DNA-mimicking brush polymers were estimated. The E_{LUMO} levels were further estimated from the E_{HOMO} levels and band gaps. The results are listed in Table 1.

References

(S1) M. Jesberger, L. Barner, M. H. Stenzel, E. Malmstrom, T. P. Davis and C. Barner-Kowollik, *J. Polym. Sci.: Part A: Polym. Chem.* 2003*,* **41**, 3847.

(S2) B. Lee, Y. -H. Park, Y. –T. Hwang, W. Oh, J. Yoon and M. Ree, *Nat. Mater.*, 2005, **4**, 147-150

(S3) J. Yoon, K. Kim, J. Kim, K. Heo, K. S. Jin, S. Jin, T. J. Shin, B. Lee, Y. Rho, B. Ahn and M. Ree, *Macromol. Res.*, 2008, **16**, 575-585.

(S4) J. Bolze, J. Kim, J. Huang, S. Rah, H. S. Youn and B. Lee, *Macromol. Res.*, 2002, **10**, 2-12.

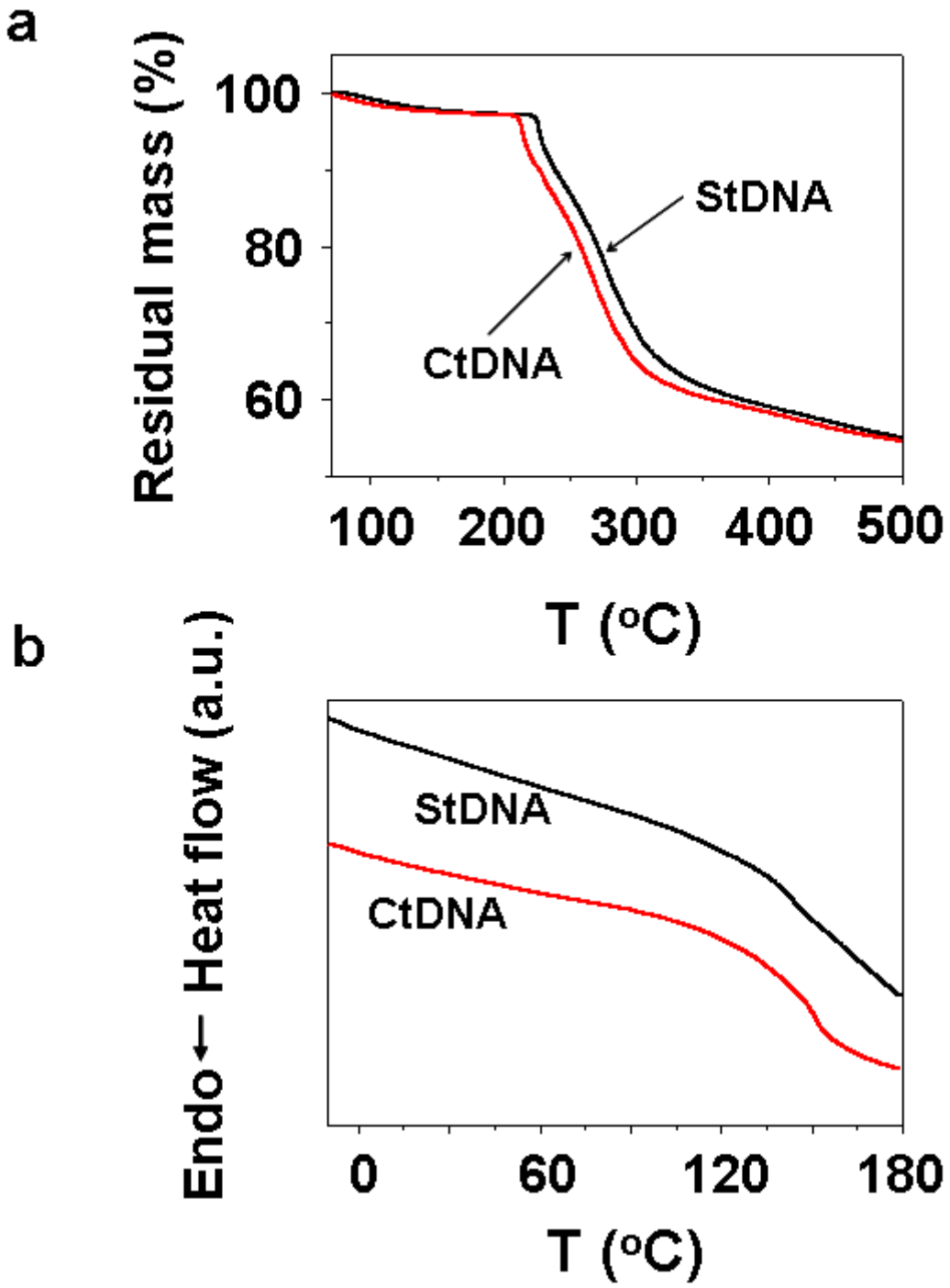

Fig. S1 Thermograms of DNAs in salt forms: (a) TGA thermograms; (b) DSC thermograms. The measurements were carried out at a rate of 10.0 ^{o}C/min under nitrogen atmosphere.

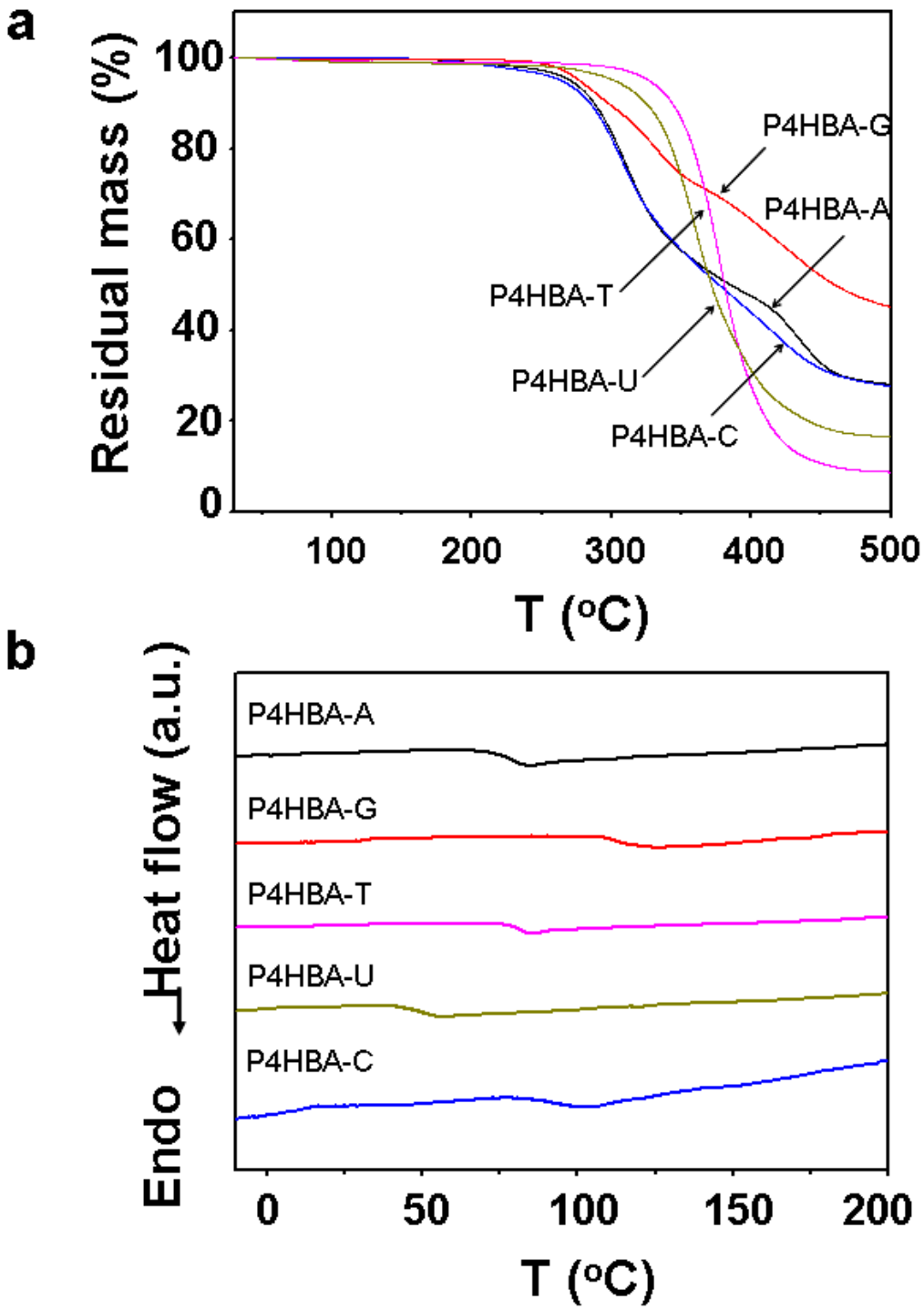

Fig. S2 Thermograms of DNA-mimicking P4HBA polymers: (a) TGA thermograms; (b) DSC thermograms. The measurements were carried out at a rate of 10.0 ^{o}C/min under nitrogen atmosphere.

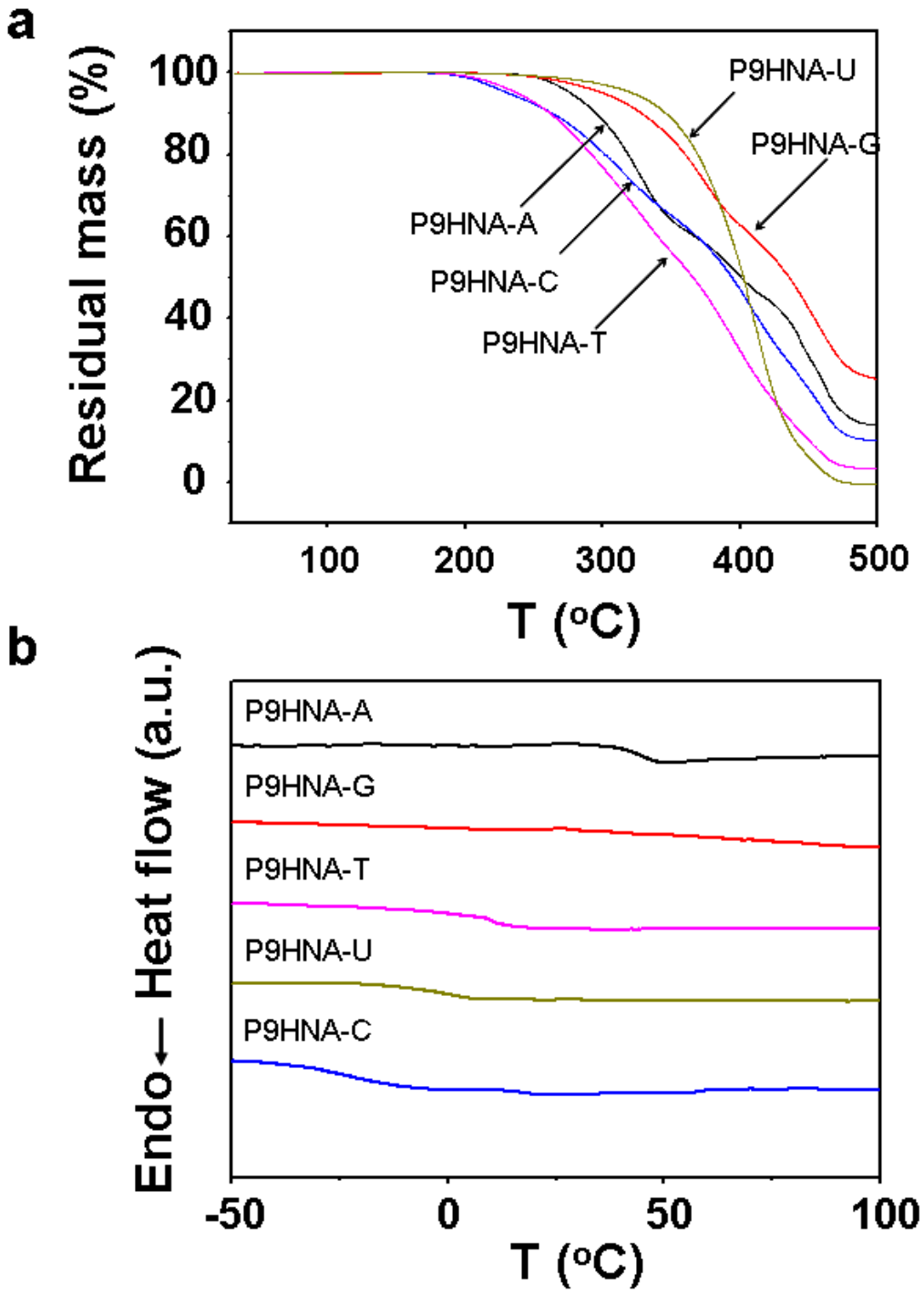

Fig. S3 Thermograms of DNA-mimicking P9HNA polymers: (a) TGA thermograms; (b) DSC thermograms. The measurements were carried out at a rate of 10.0 ^{o}C/min under nitrogen atmosphere.

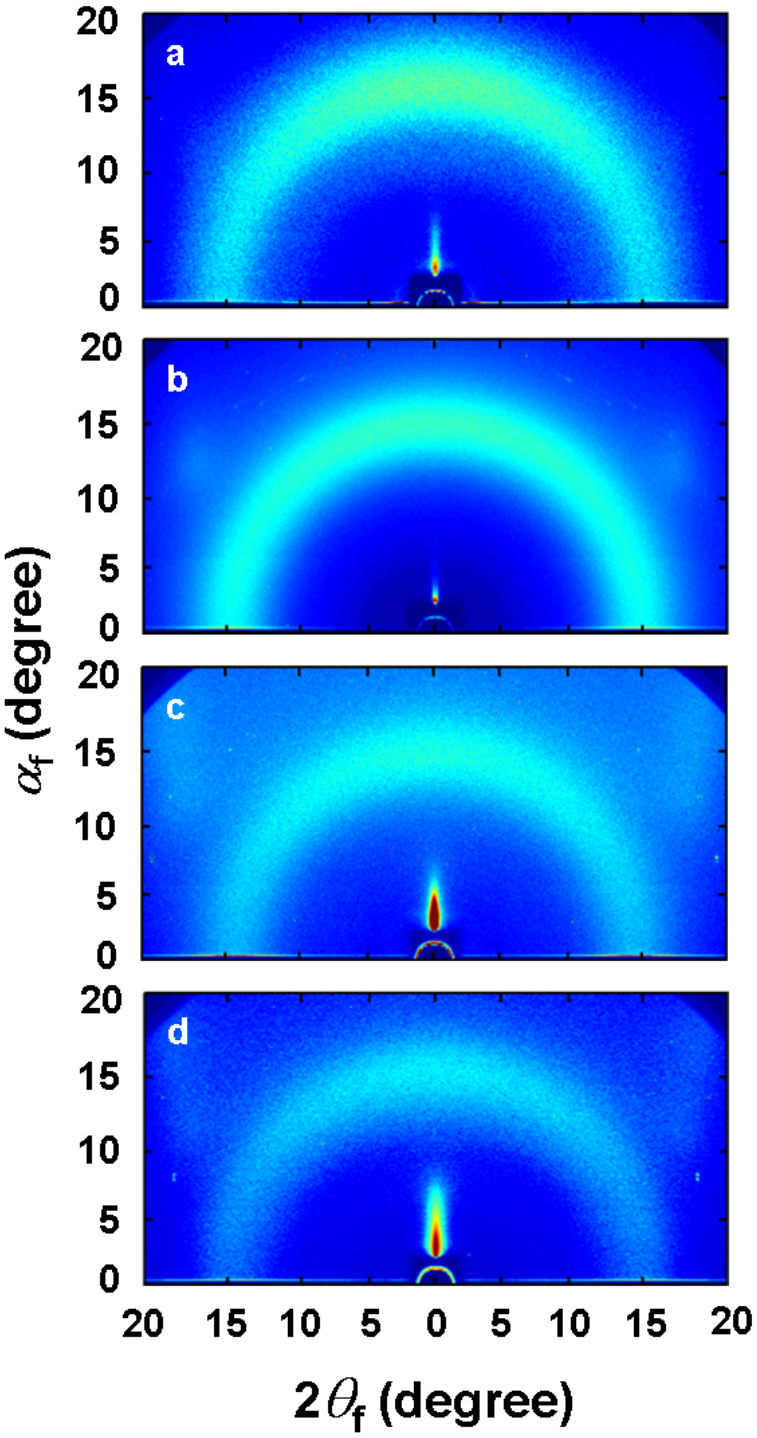

Fig. S4 Representative 2D GIXS patterns of DNA-mimicking brush polymer films measured at room temperature using an X-ray beam with a wavelength λ of 0.1110 nm: (a) P4HBA-G (as-cast), measured at $\alpha_i = 0.170°$; (b) P4HBA-T (as-cast), measured at $\alpha_i = 0.180°$; (c) P4HBA-U (as-cast), measured at $\alpha_i = 0.170°$; (d) P4HBA-C (as-cast), measured at $\alpha_i = 0.150°$.

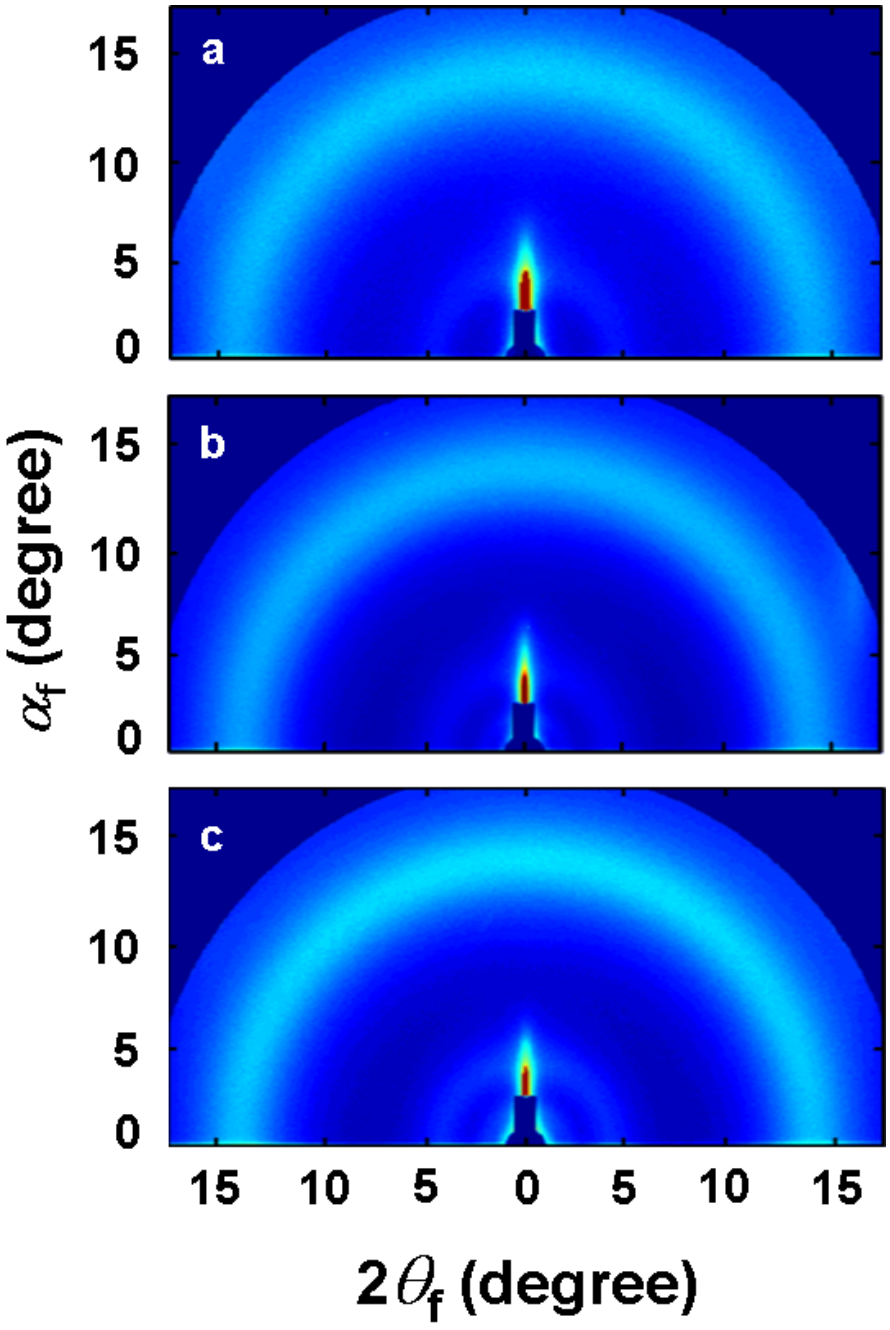

Fig. S5 Representative 2D GIXS patterns of DNA-mimicking brush polymer films measured at room temperature using an X-ray beam (λ = 0.1180 nm): (a) P9HNA-T (as-cast), measured at α_i = 0.130°; (b) P9HNA-U (as-cast), measured at α_i = 0.130°; (c) P9HNA-C (as-cast), measured at α_i = 0.140°.

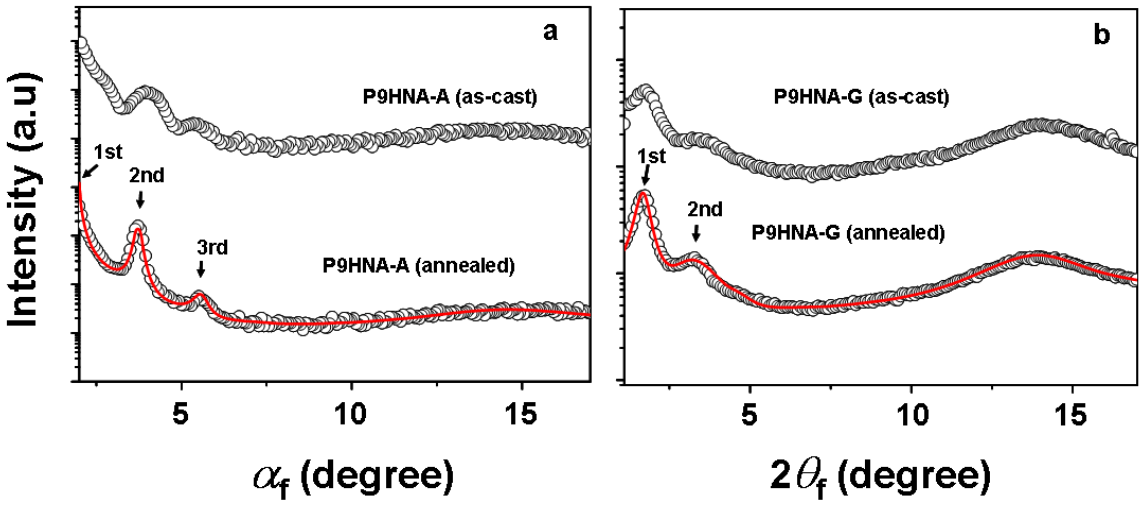

Fig. S6 One-dimensional (1D) scattering profiles extracted from the 2D GIXS patterns in Figs. 2b-e: (a) out-of-plane scattering profiles extracted along the α_f direction at $2\theta_f$ = 0° from the GIXS patterns; (b) in-plane scattering profiles extracted along the $2\theta_f$ direction at α_f =0.21° from the GIXS patterns. The black symbols are the measured data and the red solid lines were obtained by fitting the data using the GIXS formula derived with a three layer model.

Table S1 Structural parameters of the multibilayer structures developed in the solvent-annealed P9HNA-A and P9HNA-G films, which were obtained from the X-ray scattering data analysis with the GIXS formula derived for a three layer model

Film	L [a] (nm)	L_1 [b] (nm)	L_2 [c] (nm)	L_3 [d] (nm)	σ_{L1} [e] (nm)	σ_{L2} [f] (nm)	σ_{L3} [g] (nm)	g [h]	d_a [i] (nm)	$\bar{\varphi}$ [j] (deg.)	σ_φ [k] (deg.)	O_s [l]
P9HNA-A	3.43	0.51	1.05	0.82	0.02	0.10	0.03	0.062	0.45	0	5.11	0.988
P9HNA-G	3.58	1.07	0.87	0.82	0.10	0.07	0.05	0.201	0.45	90	19.3	-0.348

[a] Long period. [b] Thickness of the denser sublayer, which was originated from the interdigitated nucleobase moieties in a lateral packing. [c] Thickness of the dense sublayer, which was originated from the lateral stacks of the alkylenyl bristle linkers. [d] Thickness of the less dense sublayer originated from the lateral stacks of the polymer backbones. [e] Standard deviation of the more dense sublayer layer thickness (L_1). [f] Standard deviation of the dense sublayer layer thickness (L_2).
[g] Standard deviation of the less dense sublayer layer thickness (L_3). [h] Paracrystal distortion factor along the direction parallel to the long period of multibilayer structure. [i] Interdistance of the bristles in the multibilayer structure. [j] Mean polar angle of the orientation vector n with respect to the out-of-plane direction of the film. [k] Standard deviation of the polar angle φ. [l] Second order orientation factor. Here, the $\bar{\varphi}$, σ_φ, and O_s were determined by the analysis of the azimuthal profile extracted at $2\theta_f$= 1.85° (P9HNA-A) and $2\theta_f$ = 1.77° (P9HNA-G) from the 2D GIXS patterns in Figs. 2c and 2e respectively.

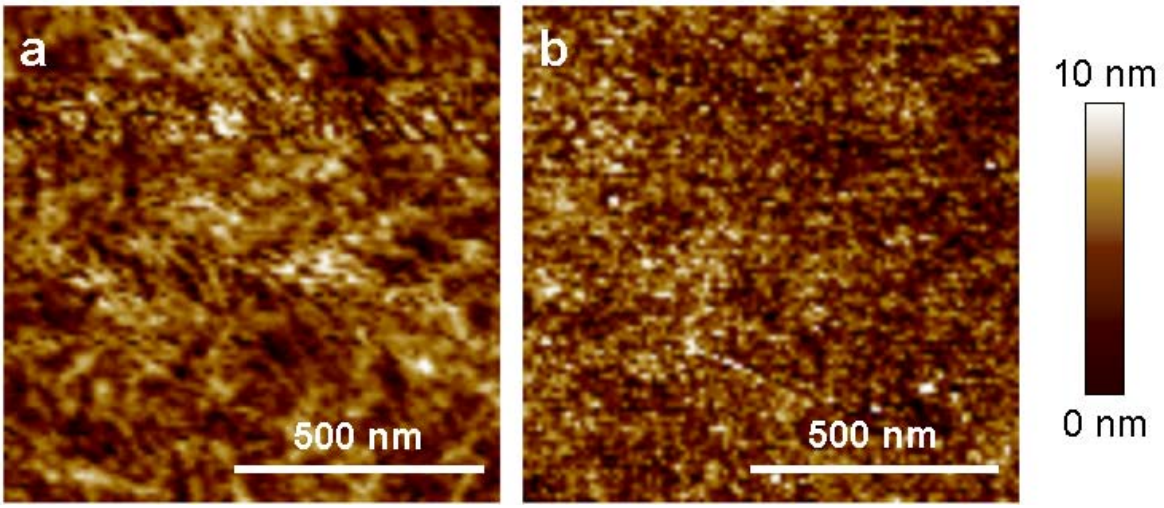

Fig. S7 Representative AFM height images (1 μm × 1 μm) of DNA films: (a) StDNA (salt form); (b) CtDNA (salt form).

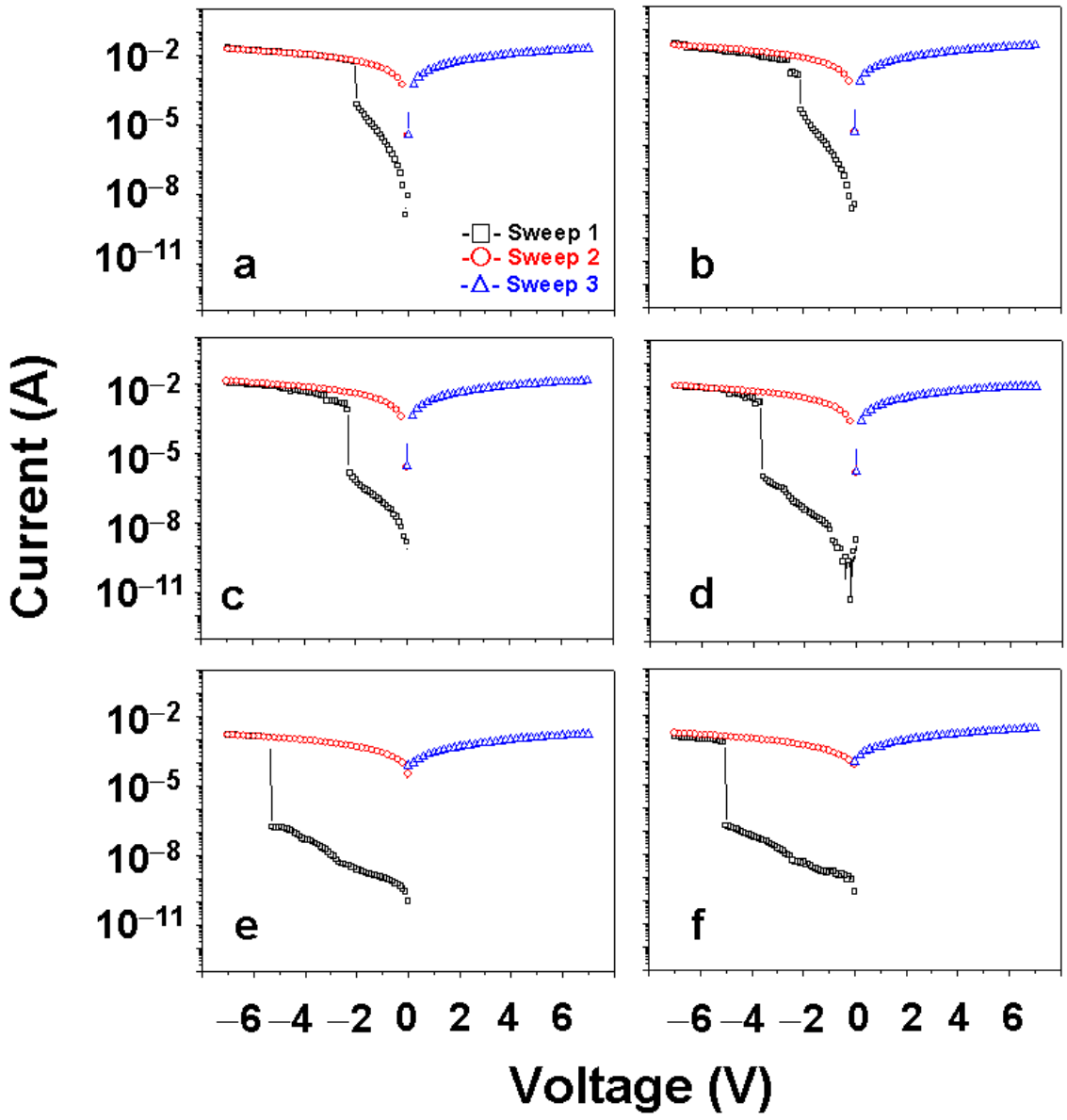

Fig. S8 Representative *I–V* curves of the Al/DNA(10 nm thick)/Al devices, which were measured in air ambient conditions with a compliance current set of 0.01 A: (a) StDNA (natural form); (b) CtDNA (natural form); (c) StDNA (salt form); (d) CtDNA (salt form); (e) StDNA-surfactant complex; (f) CtDNA-surfactant complex. The electrode contact area was 100 × 100 μm^2.

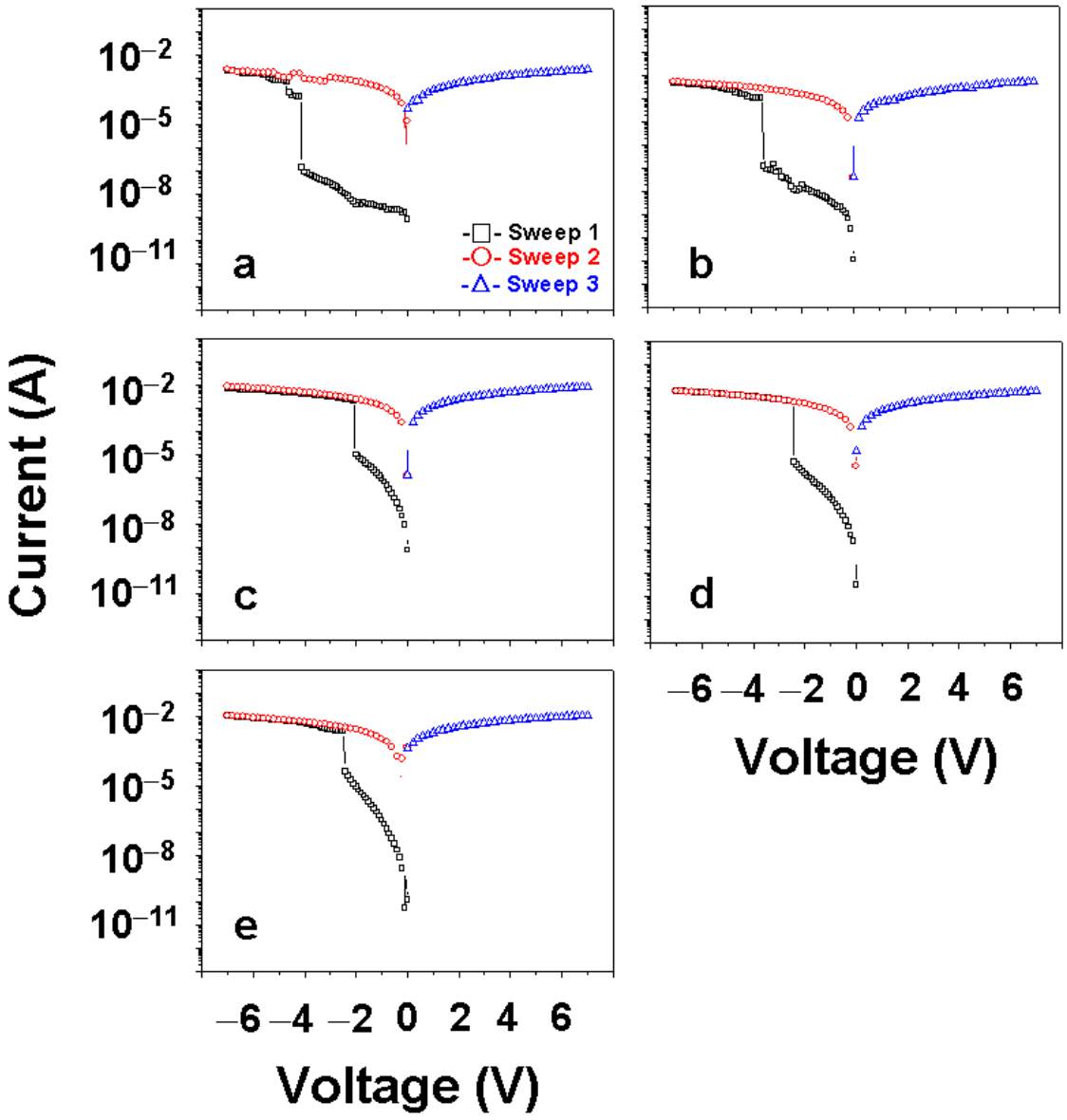

Fig. S9 Representative *I–V* curves of the Al/DNA-mimicking P4HBA polymer(10 nm thick)/Al devices, which were measured in air ambient conditions with a compliance current set of 0.01 A: (a) P4HBA-A; (b) P4HBA-G; (c) P4HBA-T; (d) P4HBA-U; (e) P4HBA-C. The electrode contact area was 100 × 100 μm^2.

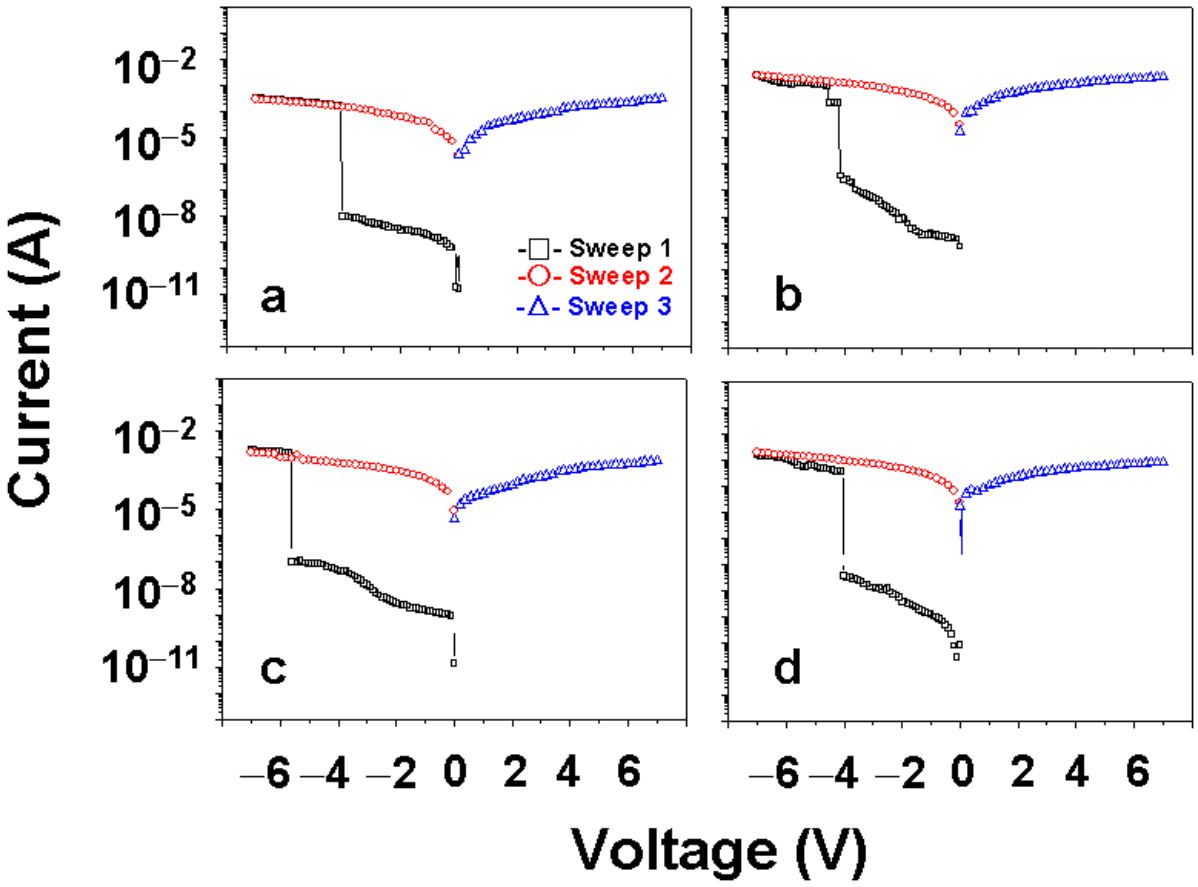

Fig. S10 Representative *I–V* curves of the Al/DNA-mimicking P9HNA polymer(10 nm thick)/Al devices, which were measured in air ambient conditions with a compliance current set of 0.01 A: (a) P9HNA-A (as-cast); (b) P9HNA-G (as-cast); (c) P9HNA-A (solvent-annealed); (d) P9HNA-G (solvent-annealed). The electrode contact area was 100 × 100 μm^2.

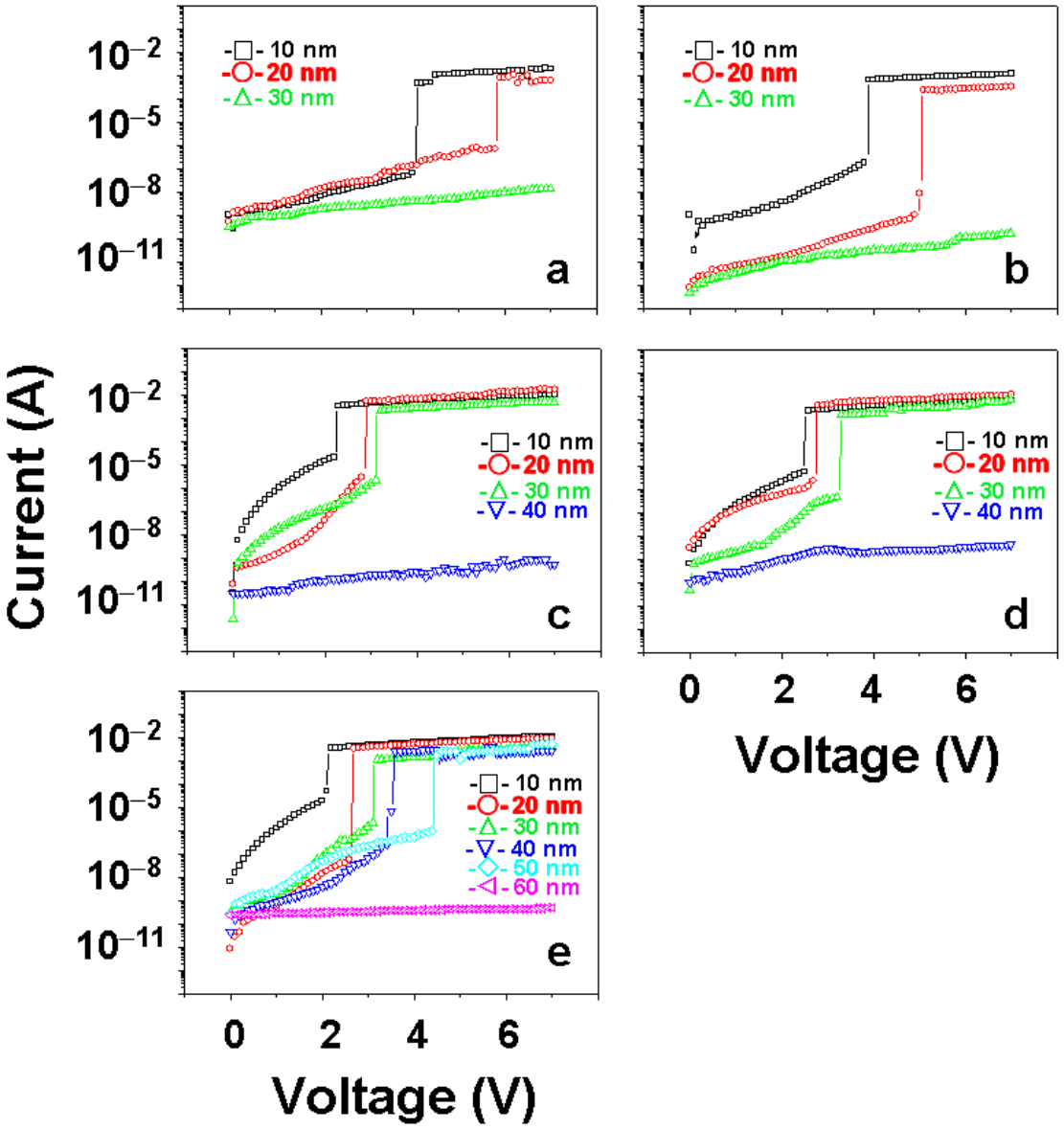

Fig. S11 Representative *I–V* curves of the Al/ DNA-mimicking P4HBA polymer/Al devices fabricated with polymer films in various thicknesses, which were measured in air ambient conditions with a compliance current set of 0.01 A: (a) P4HBA-A; (b) P4HBA-G; (c) P4HBA-T; (d) P4HBA-U; (e) P4HBA-C. The electrode contact area was 100 × 100 μm^2.

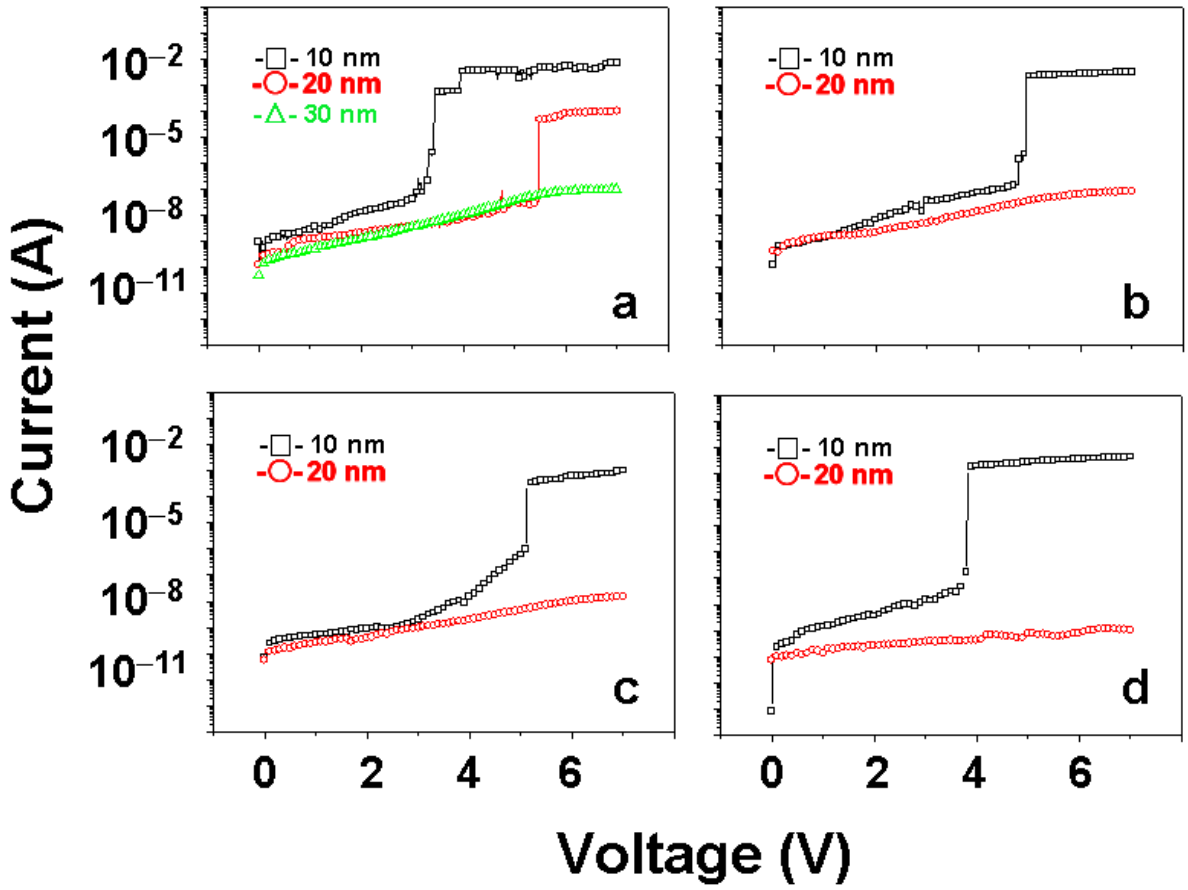

Fig. S12 Representative *I–V* curves of the Al/ DNA-mimicking P9HNA polymer/Al devices fabricated with polymer films in various thicknesses, which were measured in air ambient conditions with a compliance current set of 0.01 A: (a) P9HNA-A (as-cast); (b) P9HBA-G (as-cast); (c) P9HBA-A (solvent-annealed); (d) P9HNA-G (solvent-annealed). The electrode contact area was $100 \times 100\ \mu m^2$.

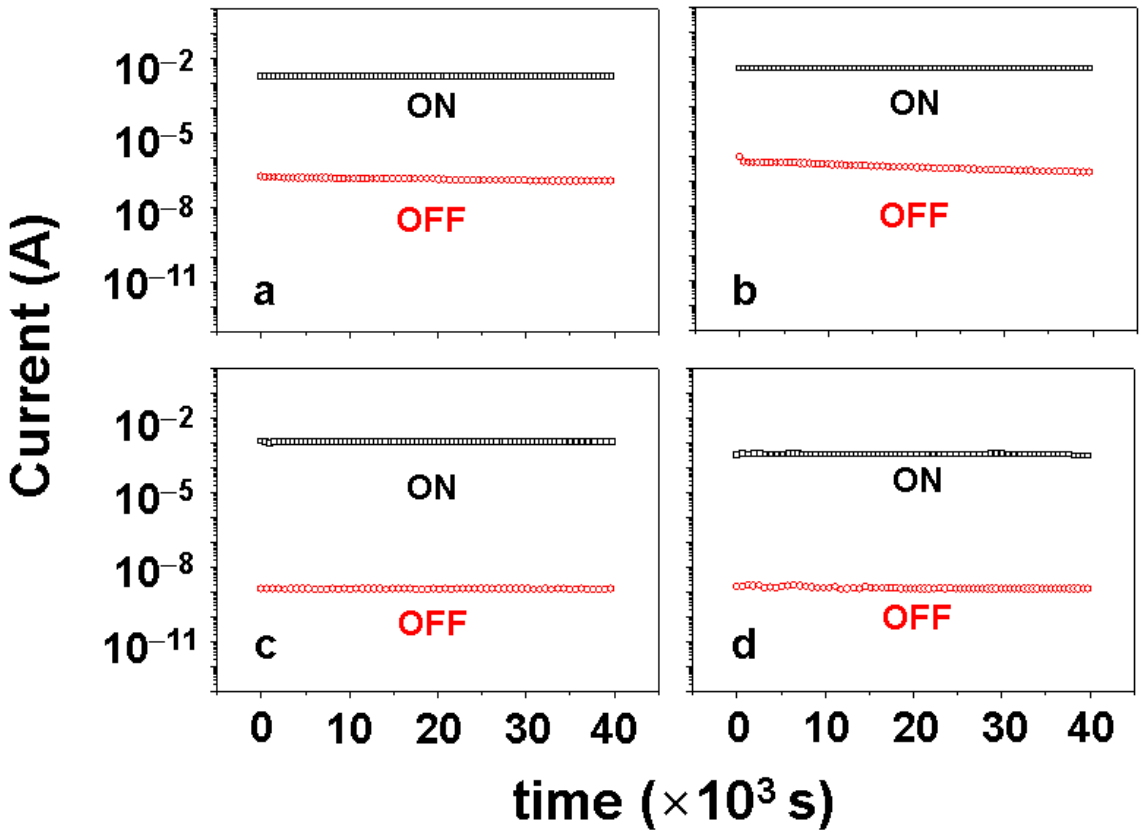

Fig. S13 Retention times of the ON- and OFF-states of the 10 nm thick DNA devices, which were measured in air ambient conditions using a reading voltage of 1.0 V and a compliance current of 0.01 A: (a) StDNA (salt form); (b) CtDNA (salt form); (c) StDNA-surfactant complex; (d) CtDNA-surfactant complex.

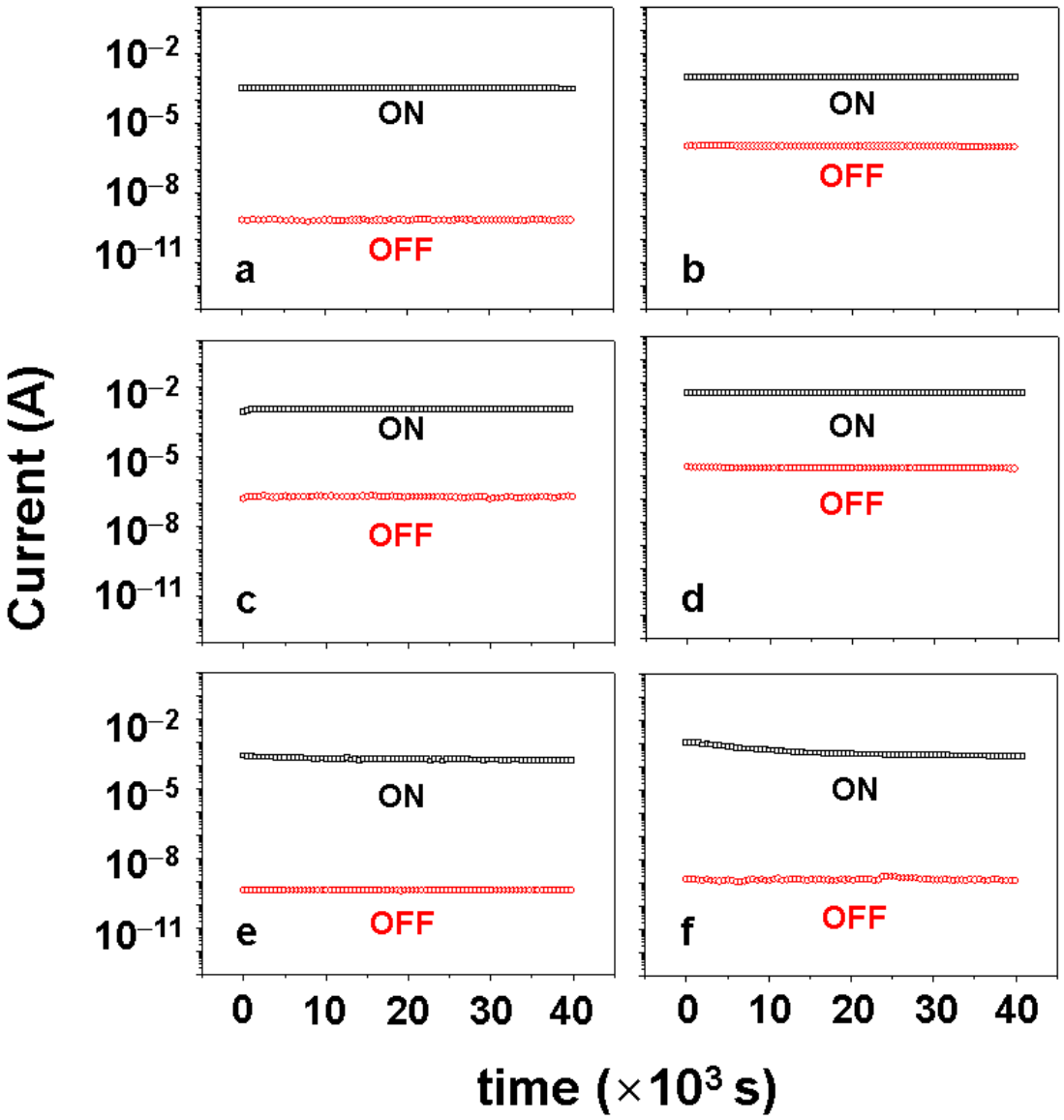

Fig. S14 Retention times of the ON- and OFF-states of the 10 nm thick DNA-mimicking brush polymer devices, which were measured in air ambient conditions using a reading voltage of 1.0 V and a compliance current of 0.01 A: (a) P4HBA-G; (b) P4HBA-T; (c) P4HBA-U; (d) P4HBA-C; (e) P9HNA-A; (f) P9HNA-G.

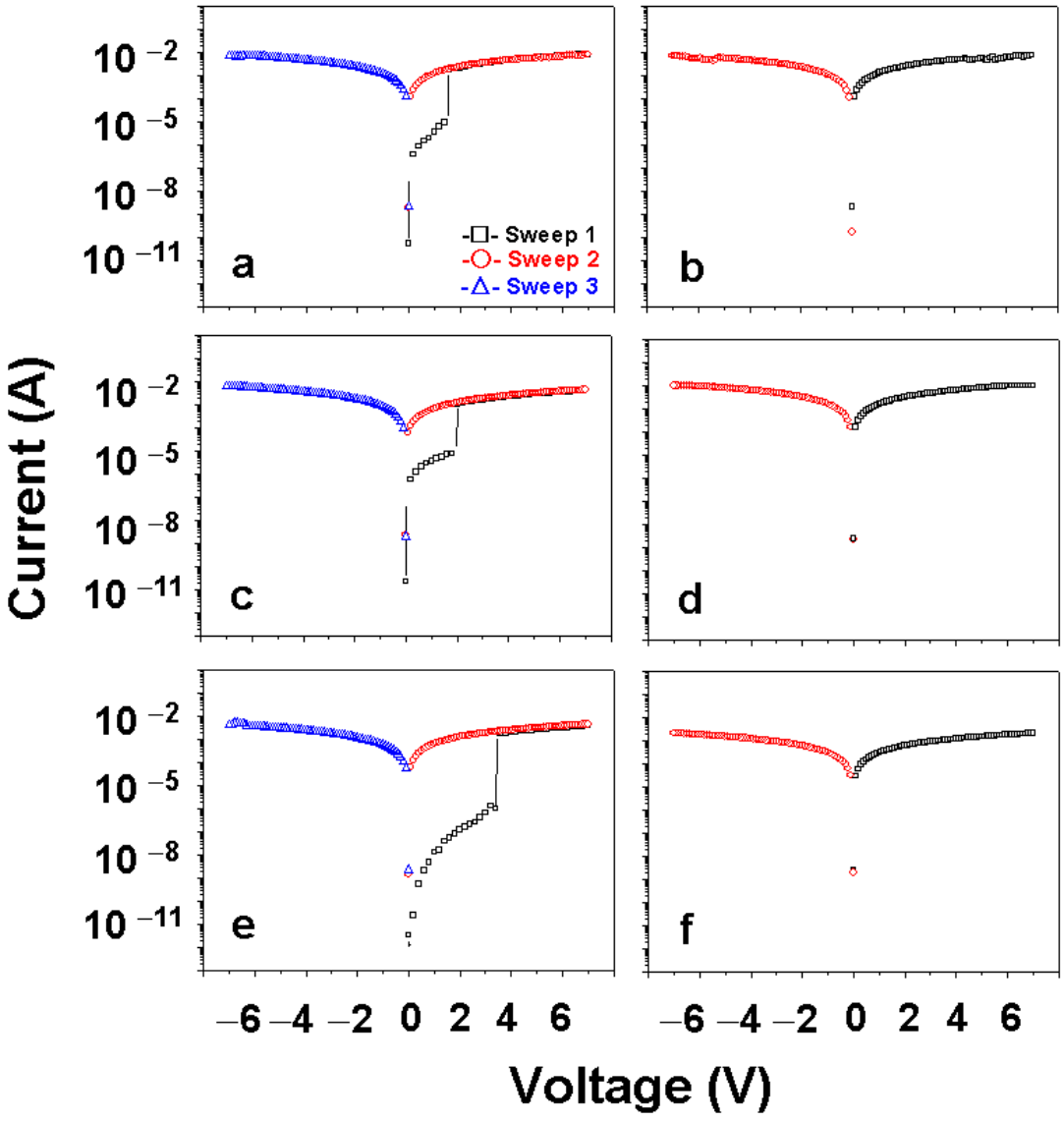

Fig. S15 Representative *I–V* curves of the Al/StDNA(10 nm thick)/Al devices, which were measured with a compliance current set of 0.01 A after stored in air in air ambient conditions for 3.5 years: (a) StDNA (natural form), an untested device cell; (b) StDNA (natural form), a device cell tested 3.5 years ago; (c) StDNA (salt form), an untested device cell; (d) StDNA (salt form), a device cell tested 3.5 years ago; (e) StDNA-surfactant complex, an untested device cell; (f) StDNA-surfactant complex, a device cell tested 3.5 years ago. The electrode contact area was 100 × 100 μm^2.

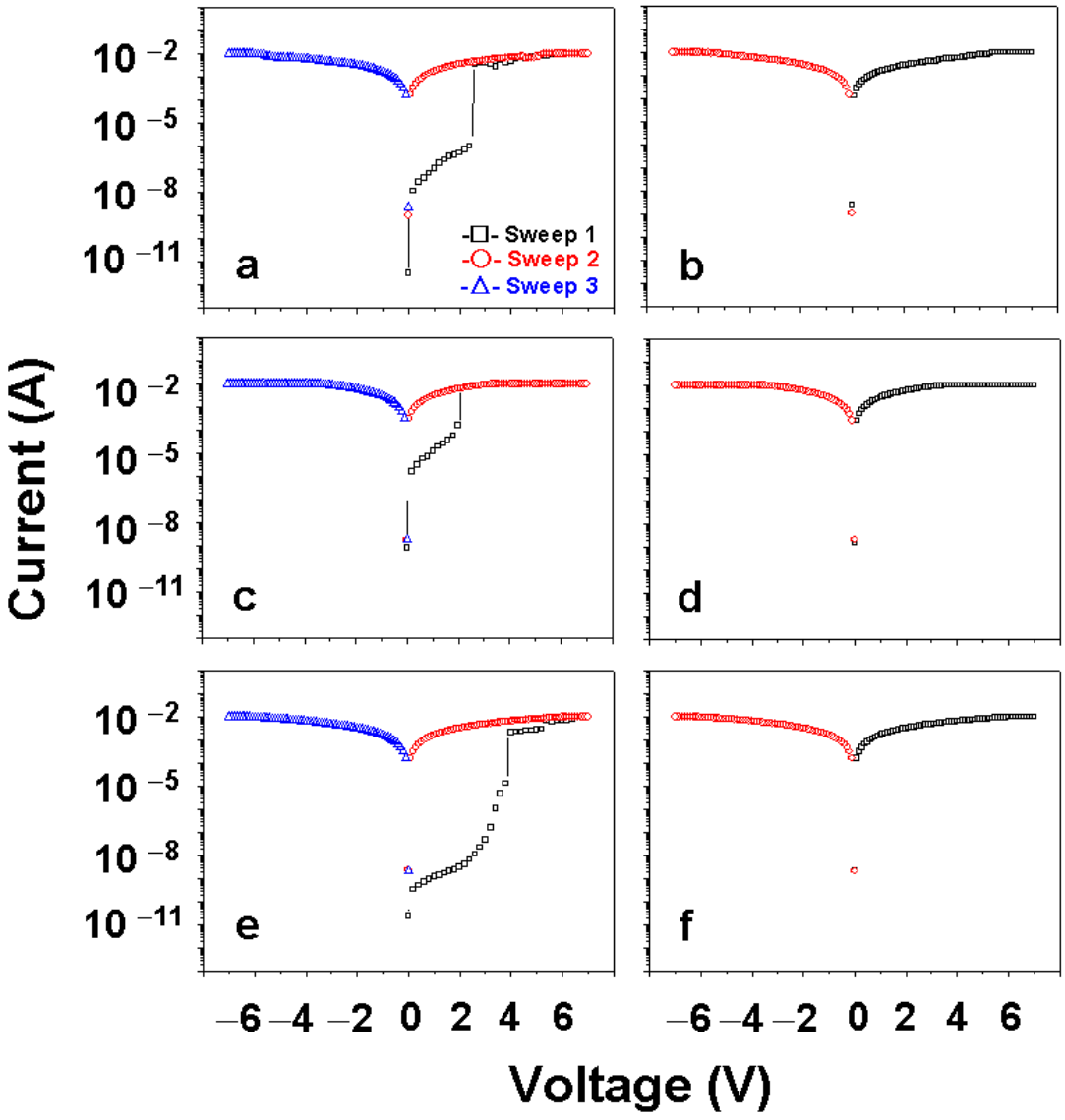

Fig. S16 Representative *I–V* curves of the Al/CtDNA(10 nm thick)/Al devices, which were measured with a compliance current set of 0.01 A after stored in air in air ambient conditions for 3.5 years: (a) CtDNA (natural form), an untested device cell; (b) CtDNA (natural form), a device cell tested 3.5 years ago; (c) CtDNA (salt form), an untested device cell; (d) CtDNA (salt form), a device cell tested 3.5 years ago; (e) CtDNA-surfactant complex, an untested device cell; (f) CtDNA-surfactant complex, a device cell tested 3.5 years ago. The electrode contact area was 100 × 100 μm^2.

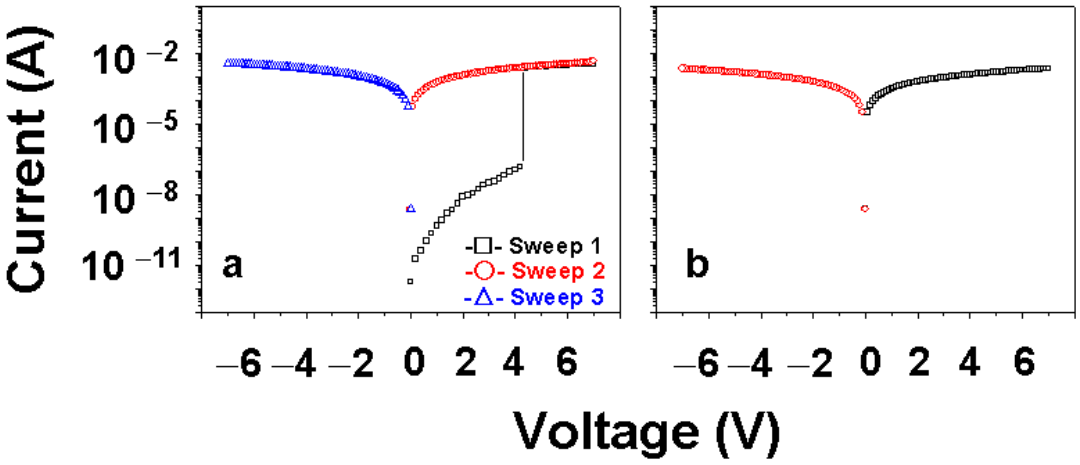

Fig. S17 Representative *I–V* curves of the Al/DNA-mimicking polymer(10 nm thick)/Al devices, which were measured with a compliance current set of 0.01 A after stored in air in air ambient conditions for 3.5 years: (a) P4HBA-A, an untested device cell; (b) P4HBA-A, a device cell tested 3.5 years ago. The electrode contact area was 100 × 100 μm^2.

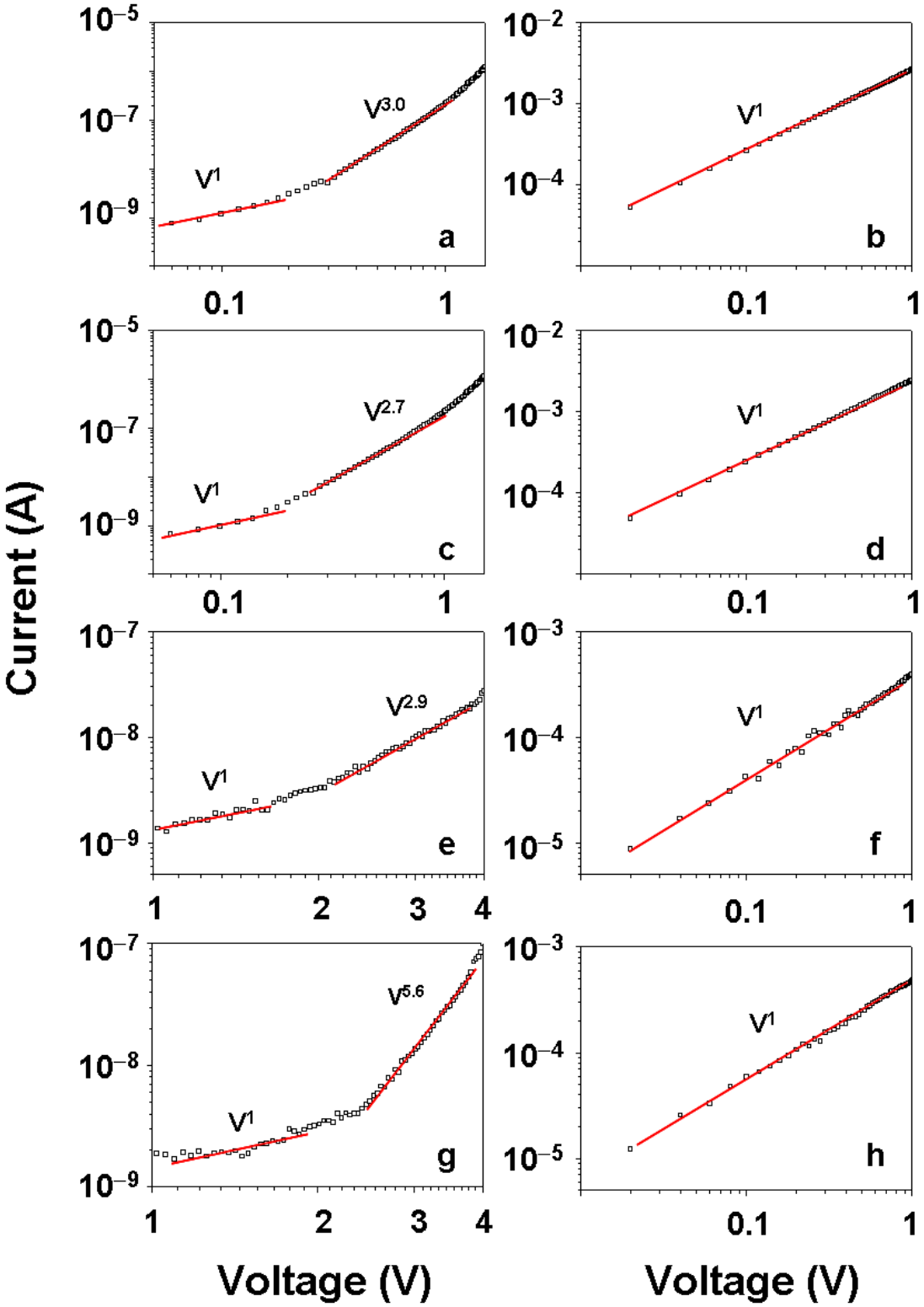

Fig. S18 *I–V* plots in the OFF-state and the ON-state of 10 nm thick DNA devices: (a, b) StDNA (salt form); (c, d) CtDNA (salt form); (e, f) StDNA-surfactant complex; (g, h) CtDNA-surfactant complex. The black symbols are the measured data and the red solid line is the fit obtained with an ohmic current conduction or a trap-limited SCLC model or their combination.

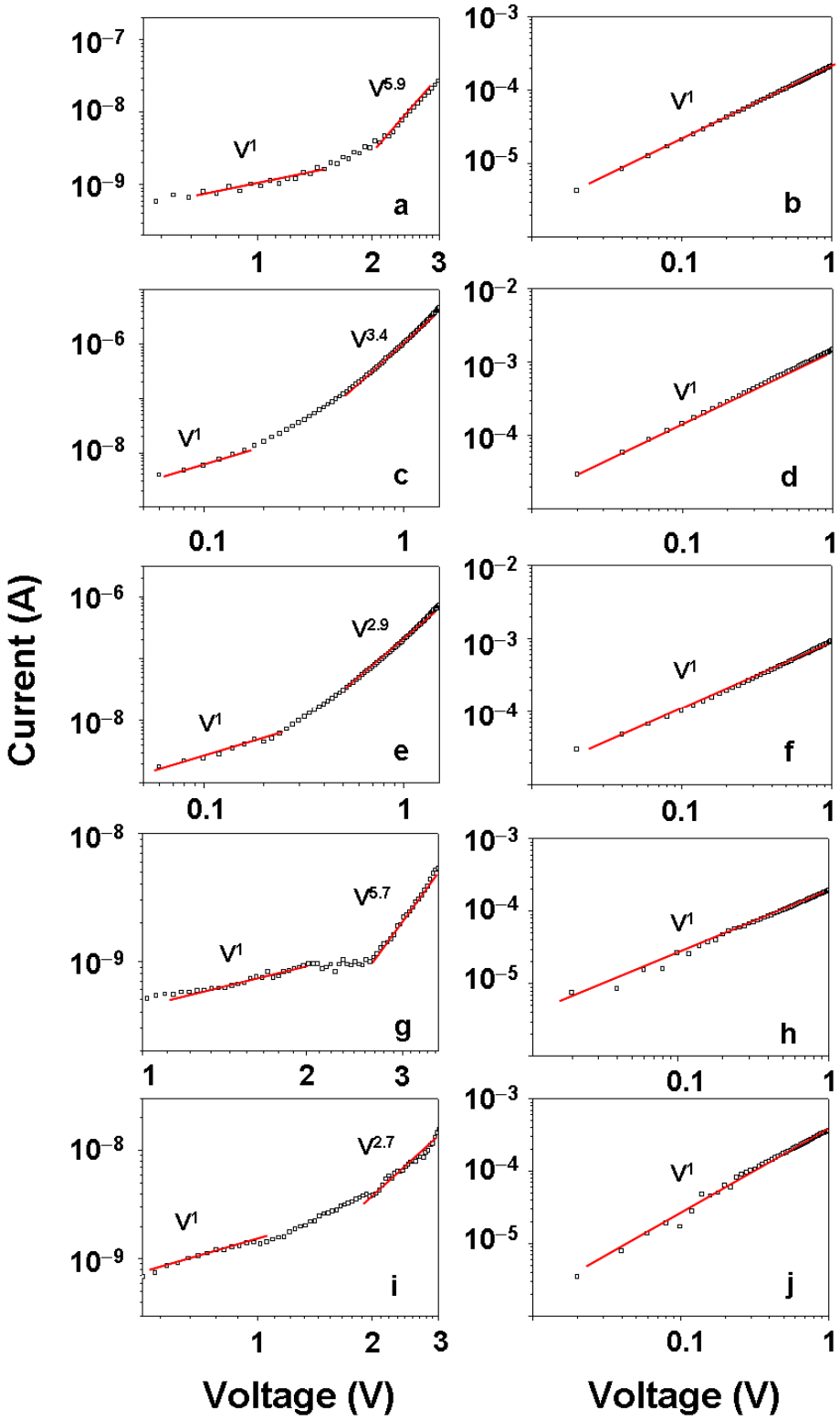

Fig. S19 *I–V* plots in the OFF-state and the ON-state of 10 nm thick DNA-mimicking polymer devices: (a, b) P4HBA-G; (c, d) P4HBA-T; (e, f) P4HBA-U; (g, h) P9HNA-A (solvent-annealed); (i, j) P9HNA-G (solvent-annealed). The black symbols are the measured data and the red solid line is the fit obtained with an ohmic current conduction or a trap-limited SCLC model or their combination.

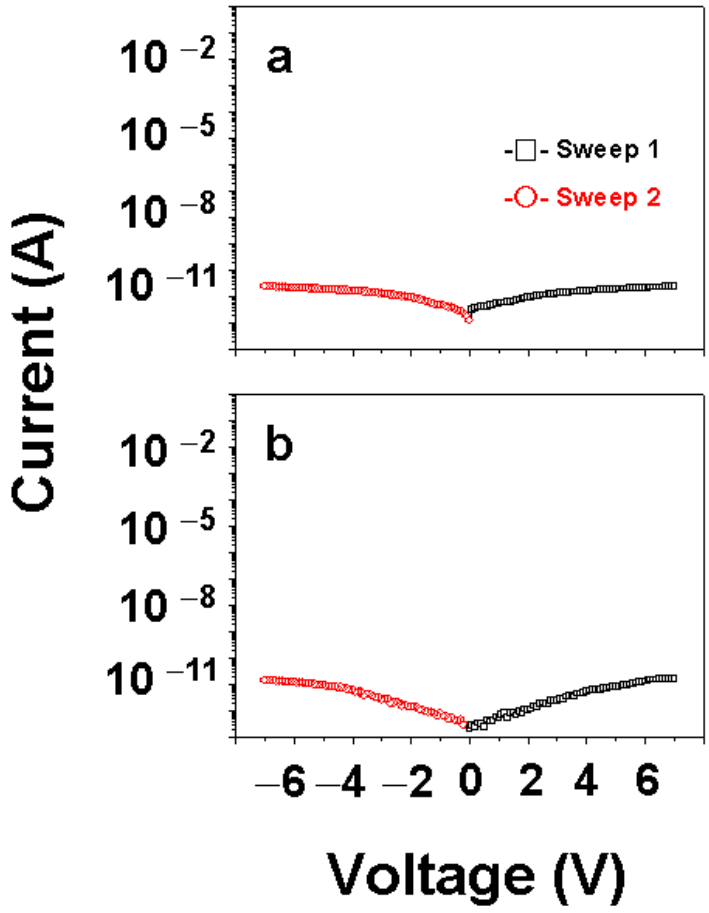

Fig. S20 Representative *I–V* curves of the Al/brush polymer without nucleobase moieties(10 nm thick)/Al devices, which were measured in air ambient conditions with a compliance current set of 0.01 A: (a) P4HBA; (b) P9HNA. The electrode contact area was 100 × 100 μm^2.

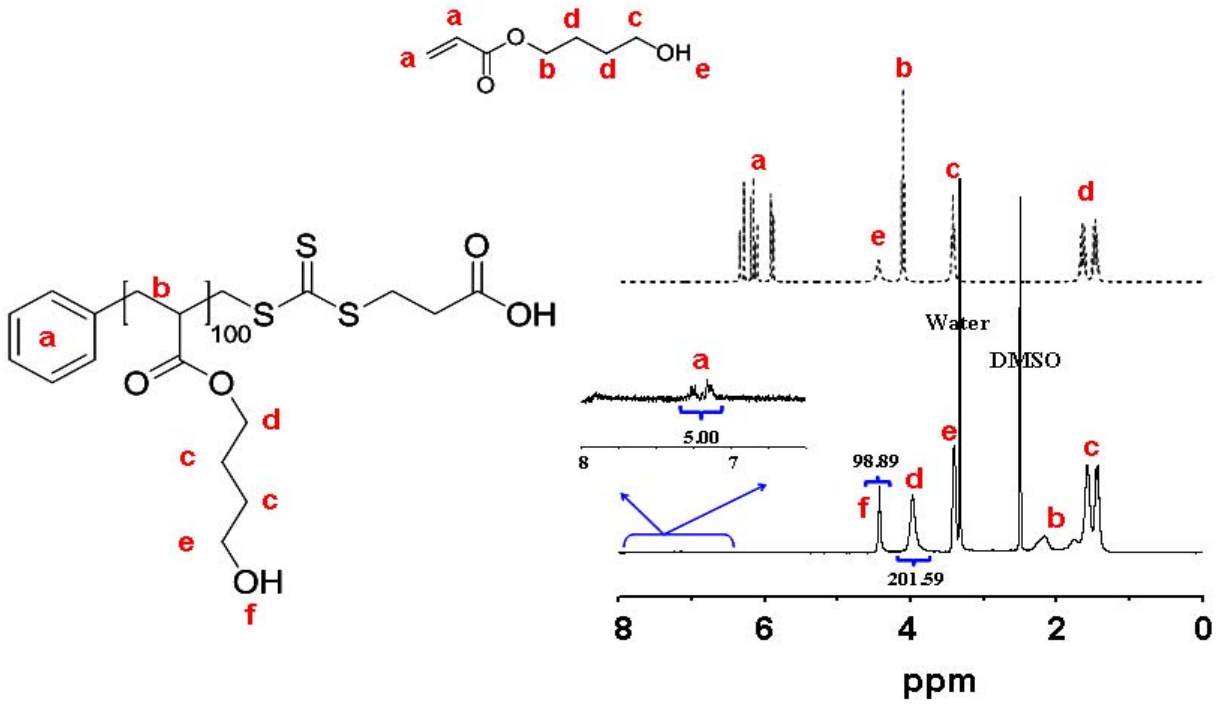

Fig. S21 ^{1}H NMR spectra of 4-hydroxybutyl acrylate (4HBA) and poly(4-hydroxybutyl acrylate) (P4HBA): (top) 4HBA, measured in $CDCl_3$; (bottom) P4HBA, measured in DMSO-d_6.

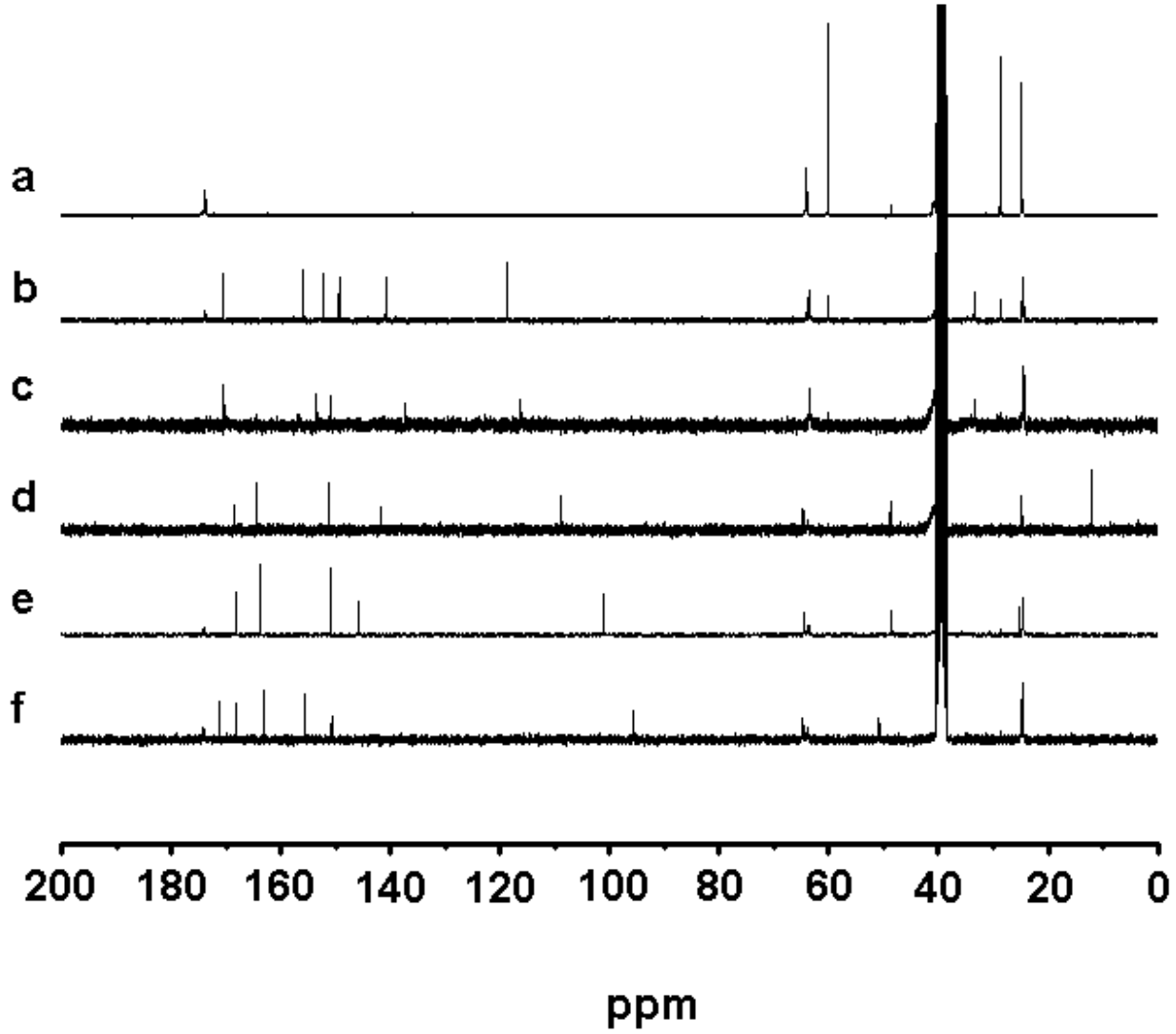

Fig. S22 ^{13}C NMR spectra of brush polymers measured in DMSO-d_6: (a) P4HBA; (b) P4HBA -A; (c) P4HBA -G; (d) P4HBA -T; (e) P4HBA -U; (f) P4HBA -C.

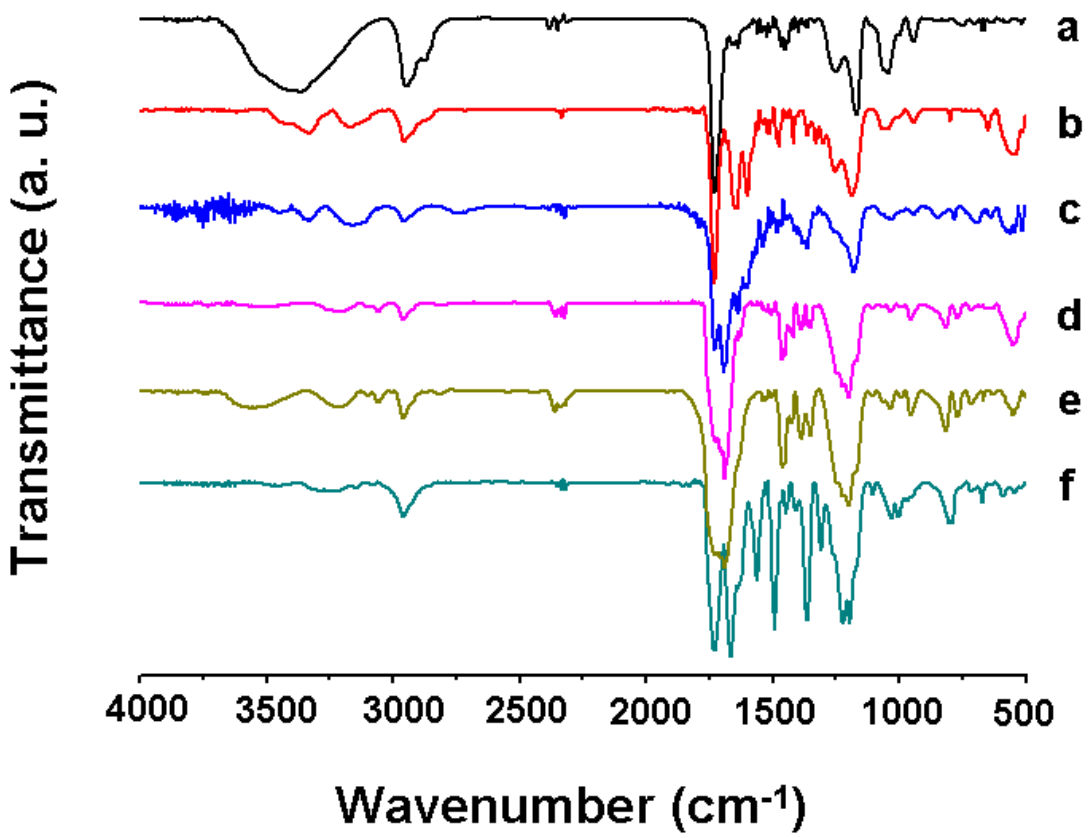

Fig. S23 IR spectra of brush polymers measured (film on KBr pellet): (a) P4HBA; (b) P4HBA -A; (c) P4HBA -G; (d) P4HBA -T; (e) P4HBA -U; (f) P4HBA -C.

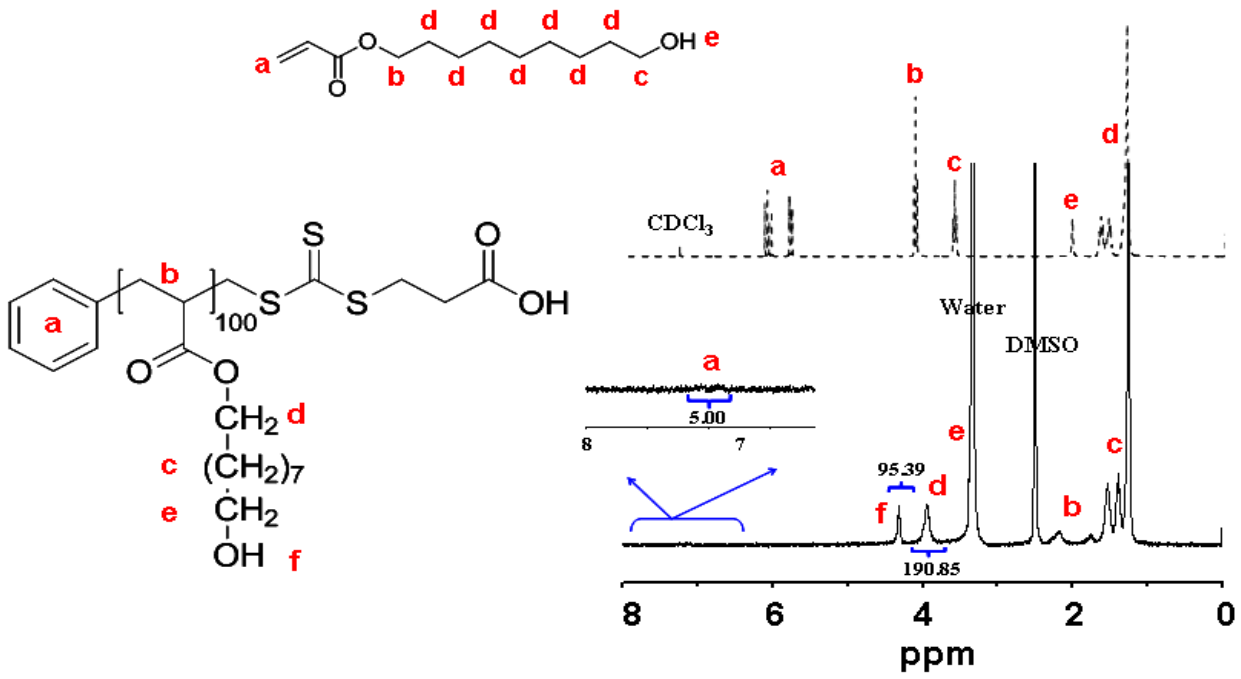

Fig. S24 ^{1}H NMR spectra of 9-hydroxynonyl acrylate (9HNA) and poly(9-hydroxynonyl acrylate) (P9HNA): (top) 9HNA, measured in $CDCl_3$; (bottom) P9HNA, measured in DMSO-d_6.

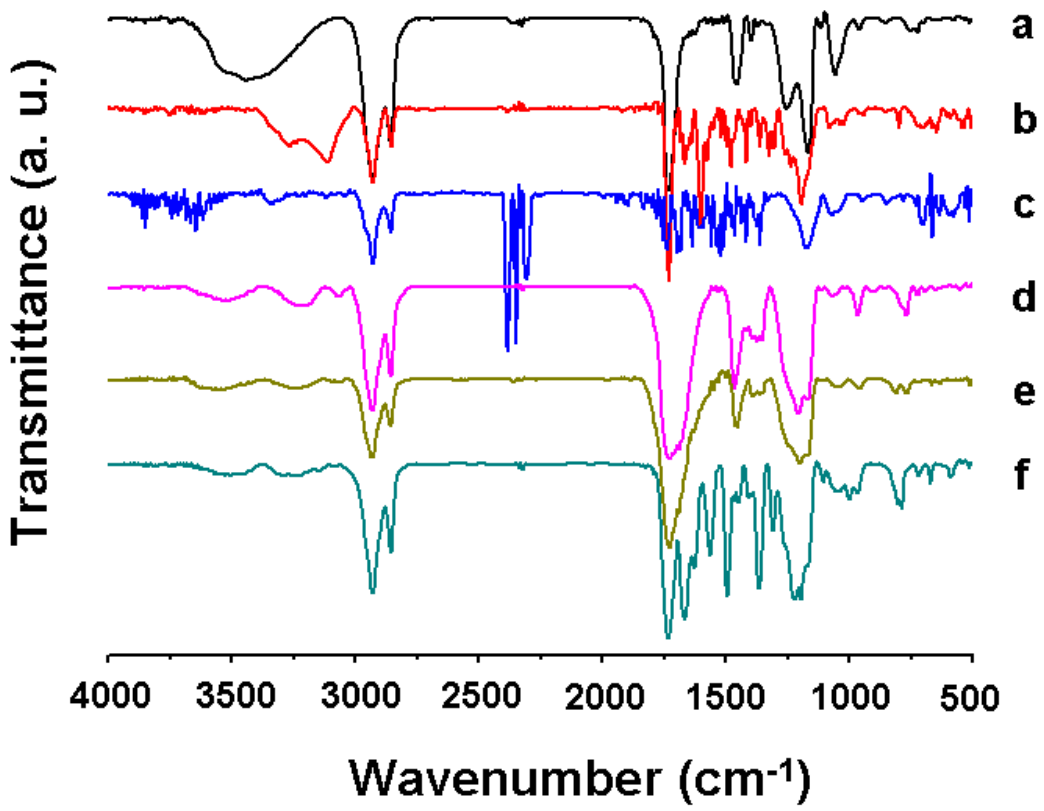

Fig. S25 IR spectra of brush polymers measured (film on KBr pellet): (a) P9HNA; (b) P9HNA -A; (c) P9HNA -G; (d) P9HNA -T; (e) P9HNA -U; (f) P9HNA -C.

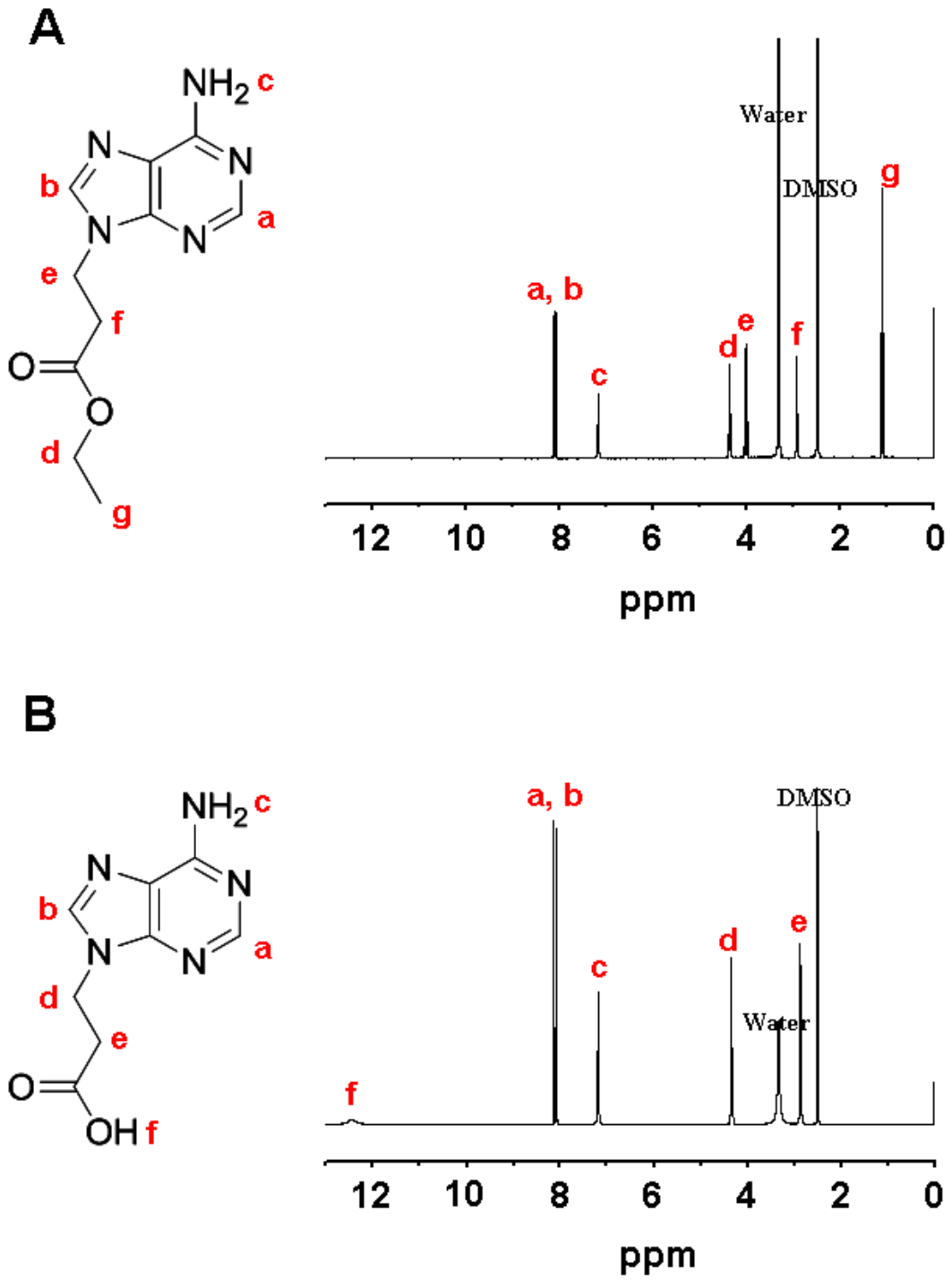

Fig. S26 ^{1}H NMR spectra of adenine derivatives measured in DMSO-d_6: (A) ethyl 3-(9-adeninyl) propionate; (B) 3-(9-adeninyl)propionic acid.

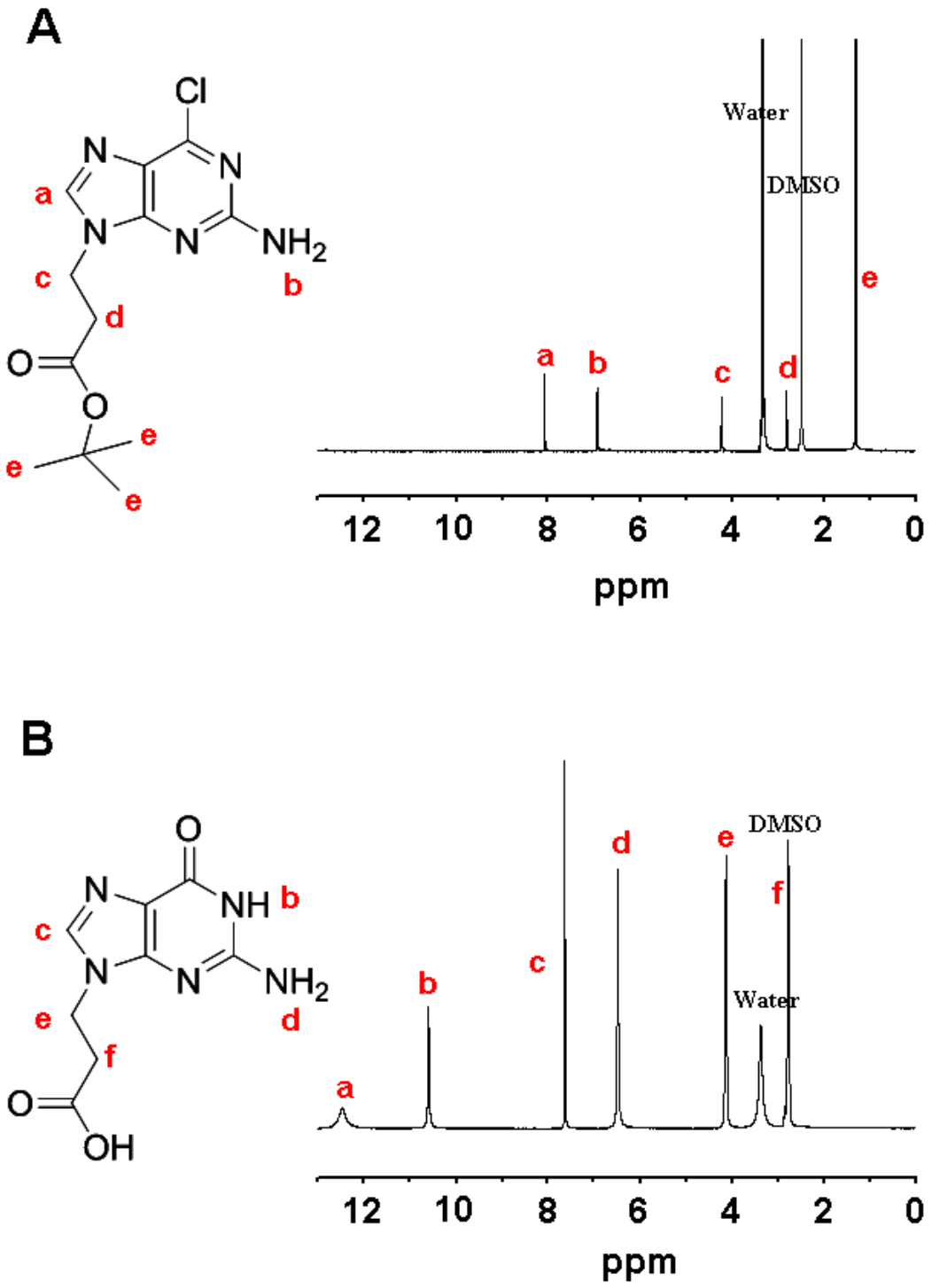

Fig. S27 ^{1}H NMR spectra of guanine derivatives measured in DMSO-d_6: (A) 2-amino-9-(2-tert-butoxycarbonylethyl)-6-chloropurine; (B) 9-(2-carboxyethyl)guanine.

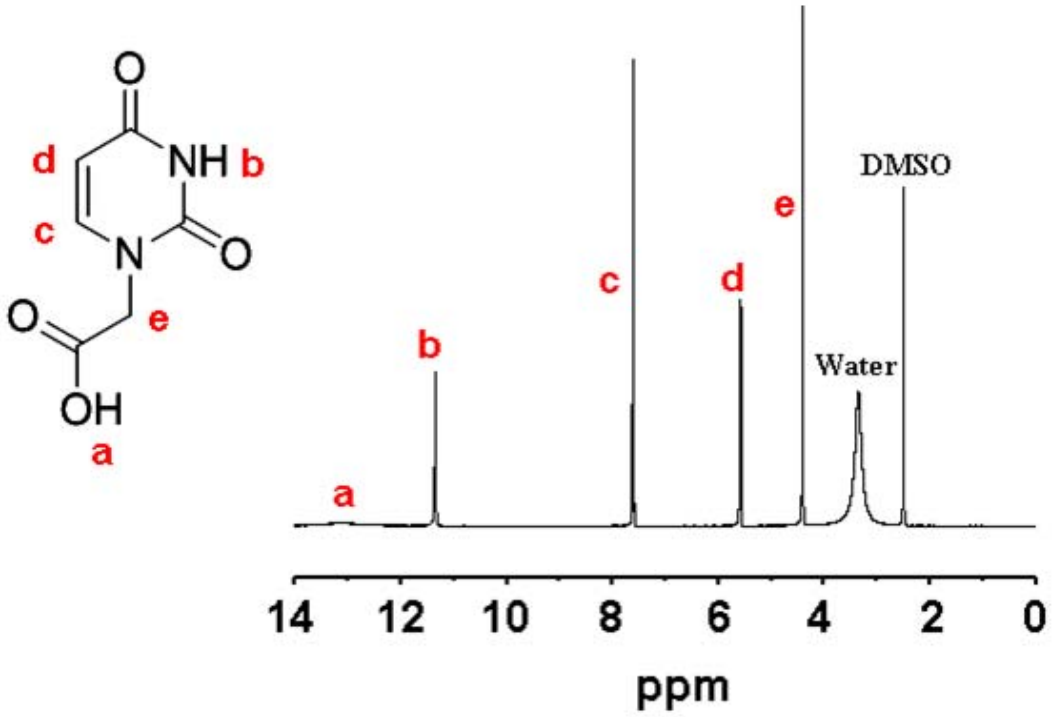

Fig. S28 ^{1}H NMR spectrum of 1-carboxymethyluracil measured in DMSO-d_6.

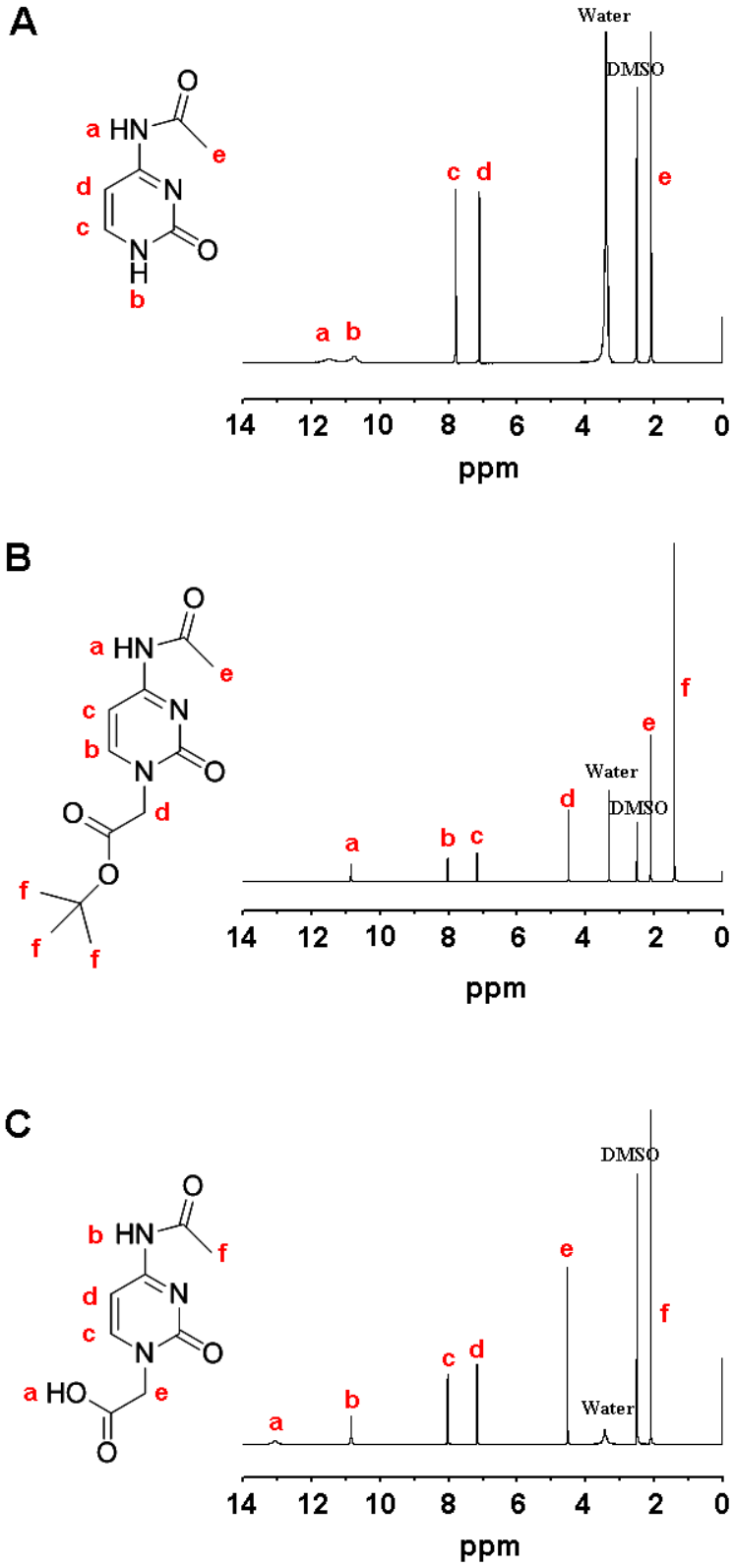

Fig. S29 ^{1}H NMR spectra of cytosine derivatives measured in DMSO-d_6: (A) N^4-acetylcytosine; (B) N^4-acetyl-1-tert-butoxycarbonylmethylcytosine; (C) N^4-acetyl-1-carboxymethylcytosine.

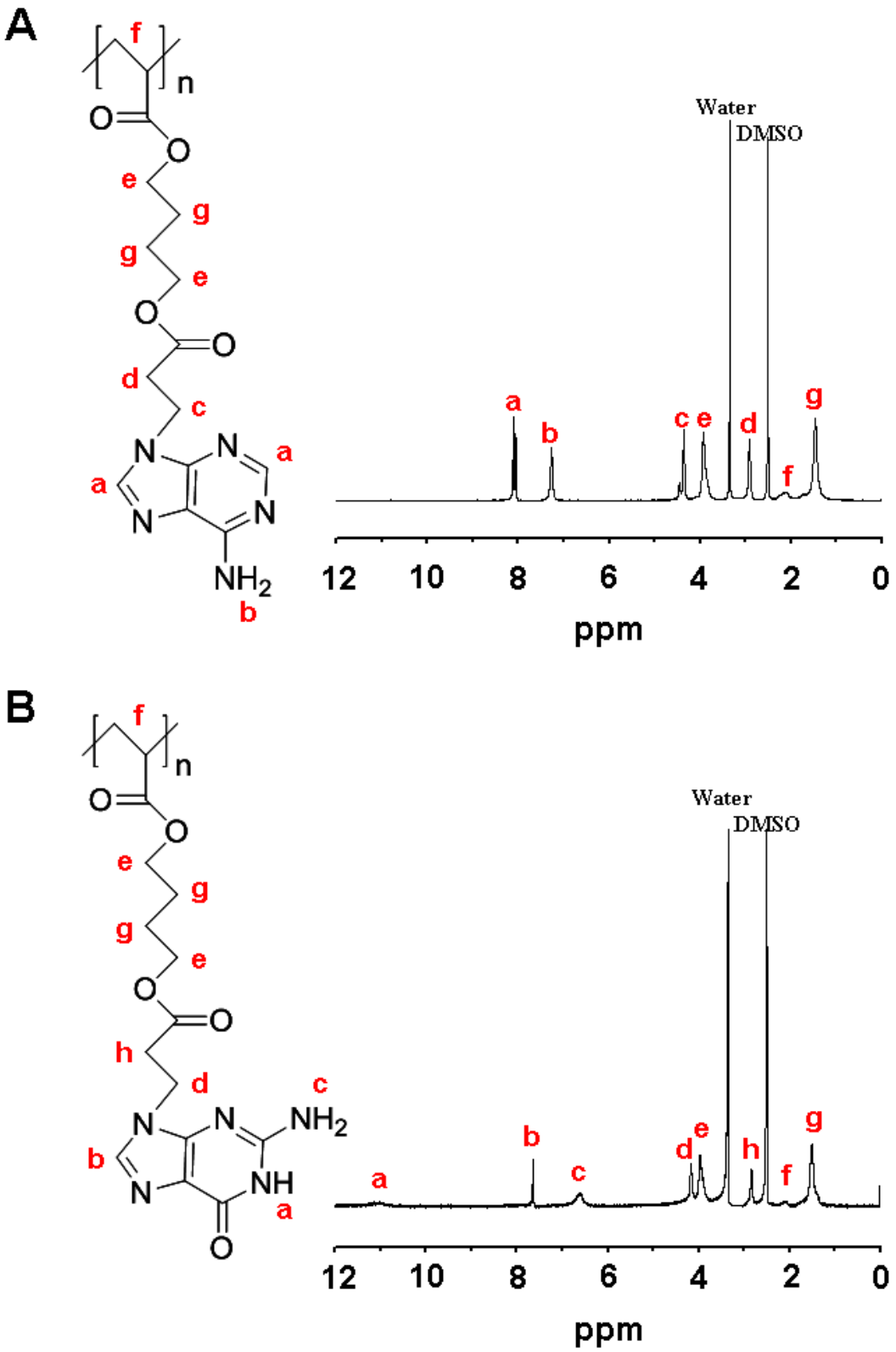
A
f
n
O
O
e
g
g
e
O
O
d
c
N
N
a
a
N
N
NH2
b
Water
DMSO
a
b
c e
d
f
g
12
10
8
6
4
2
0
ppm
B
f
n
O
O
e
g
g
e
O
O
h
d
c
N
N
NH2
b
N
NH
a
O
Water
DMSO
a
b
c
d
e
h
f
g
12
10
8
6
4
2
0
ppm

C

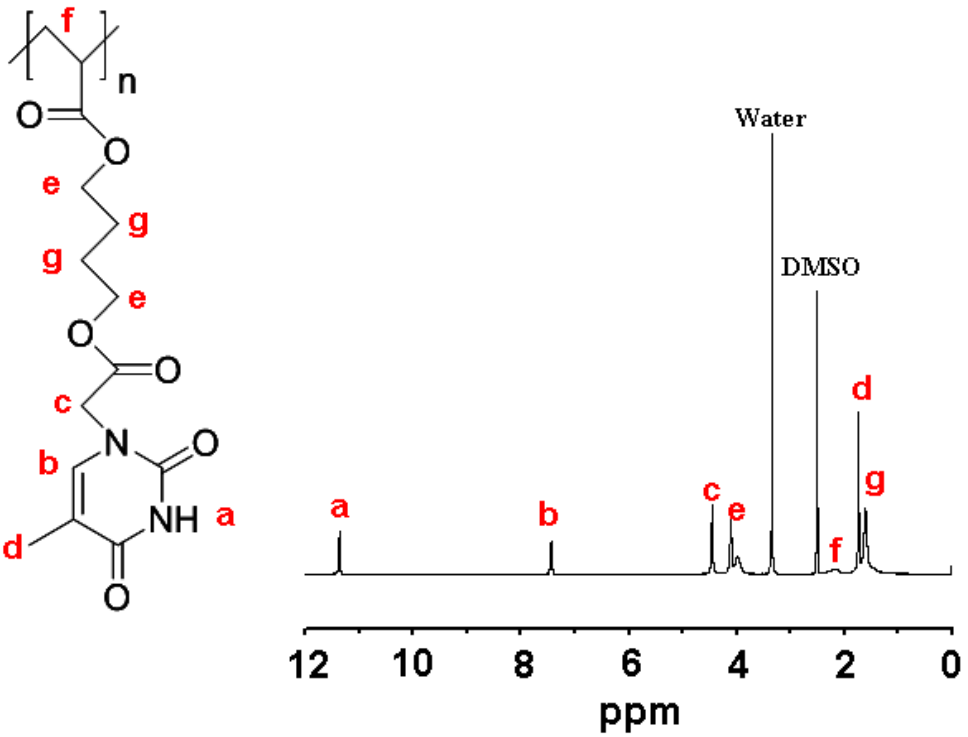
f
n
O
O
e
g
g
e
O
O
c
N
O
b
NH
a
d
O
Water
DMSO
d
g
a
b
c
e
f
12
10
8
6
4
2
0
ppm

D

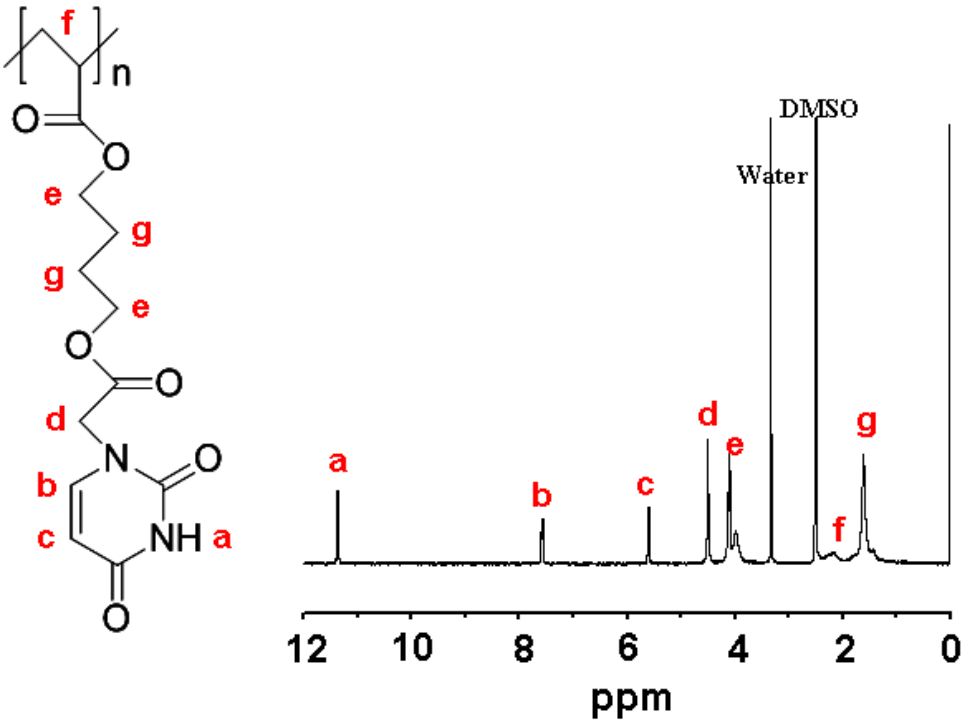
f
n
O
O
e
g
g
e
O
O
d
N
O
b
NH
a
c
O
DMSO
Water
d
e
g
a
b
c
f
12
10
8
6
4
2
0
ppm

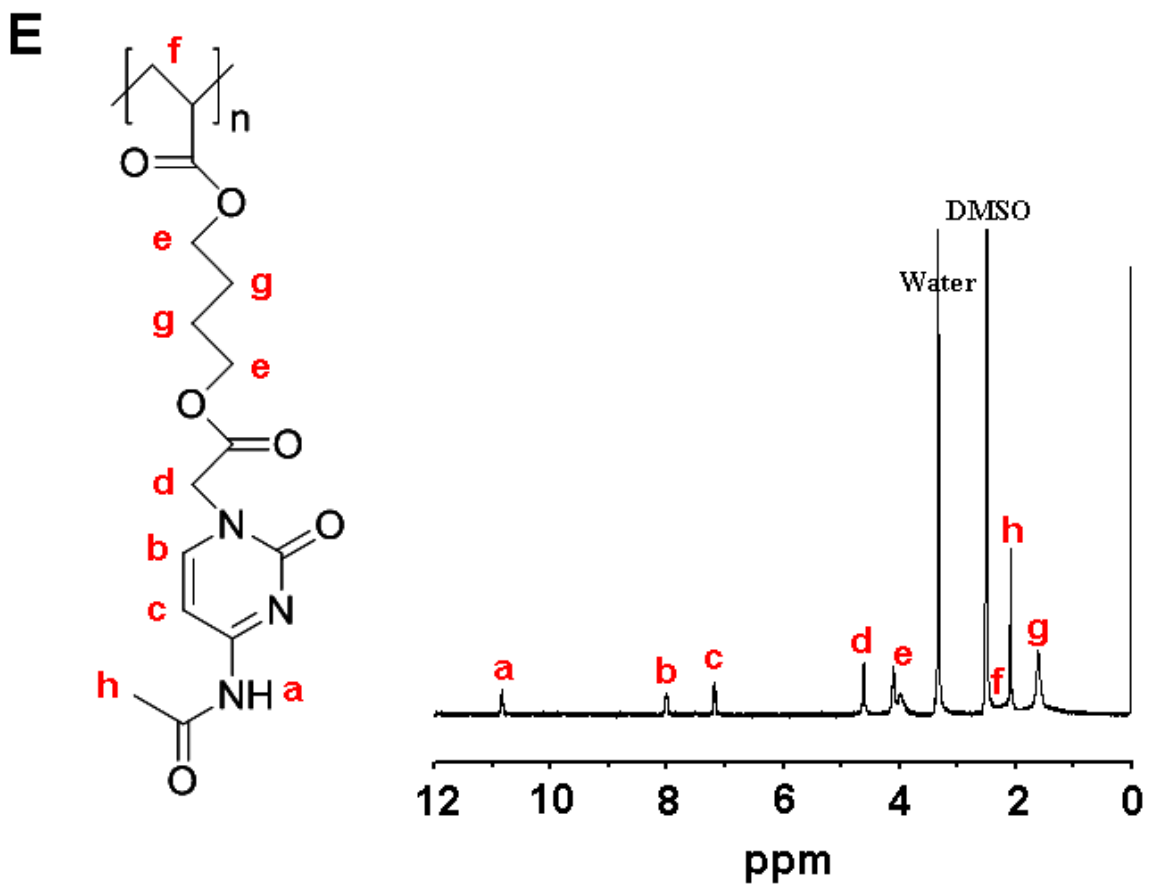

Fig. S30 ^{1}H NMR spectra of DNA-mimicking brush polymers measured in DMSO-d_6: (A) P4HBA-A; (B) P4HBA-G; (C) P4HBA-T; (D) P4HBA-U; (E) P4HBA-C.

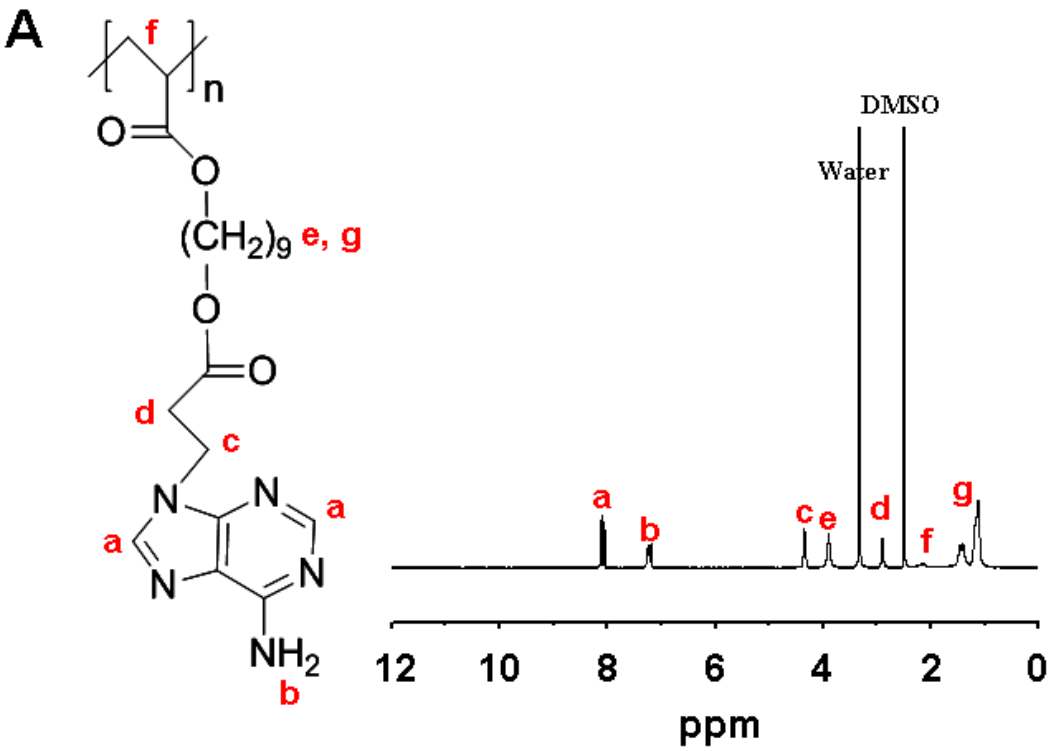
A
f
n
O
O
(CH2)9
e, g
O
O
d
c
N
N
a
a
N
N
NH2
b
DMSO
Water
a
b
c
e
d
f
g
12
10
8
6
4
2
0
ppm

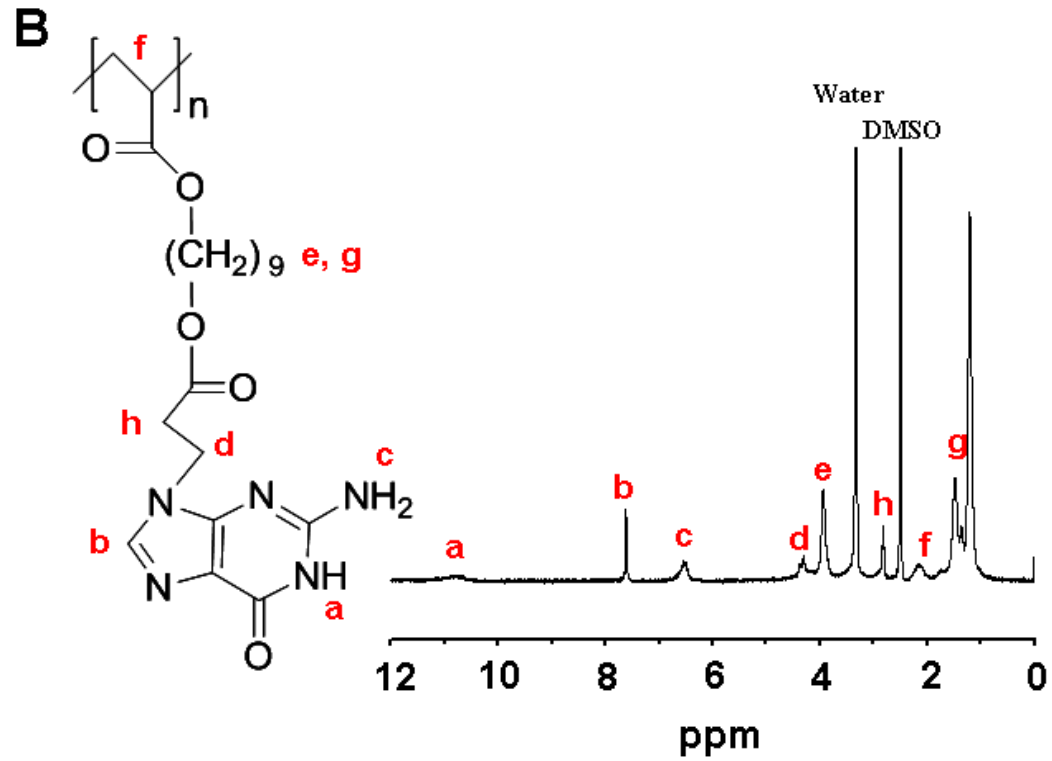
B
f
n
O
O
(CH2)9
e, g
O
O
h
d
c
N
N
NH2
b
N
NH
a
O
Water
DMSO
a
b
c
d
e
h
f
g
12
10
8
6
4
2
0
ppm

C

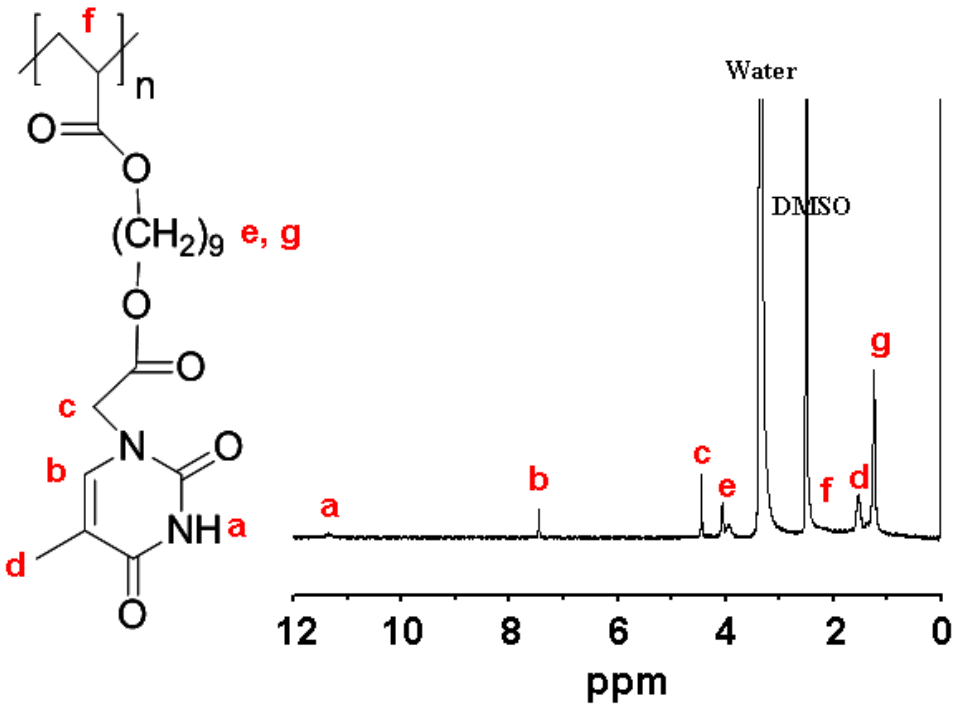
f
n
O
O
(CH2)9
e, g
O
O
c
N
O
b
NH
a
d
O
Water
DMSO
g
c
b
e
f
d
a
12
10
8
6
4
2
0
ppm

D

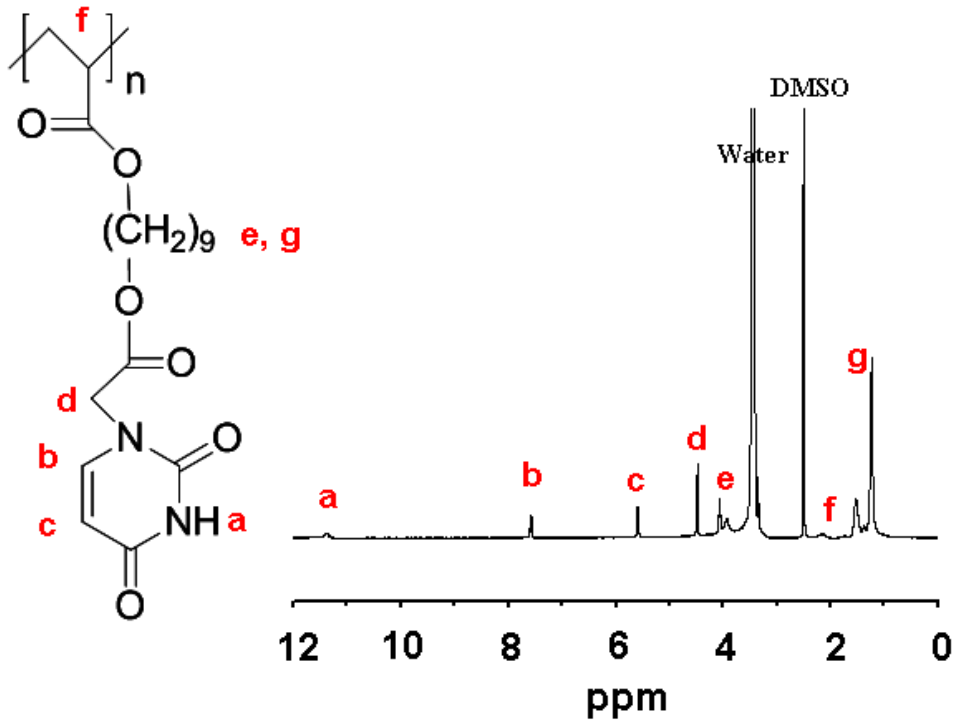
f
n
O
O
(CH2)9
e, g
O
O
d
N
O
b
NH
a
c
O
DMSO
Water
g
d
b
c
e
a
f
12
10
8
6
4
2
0
ppm

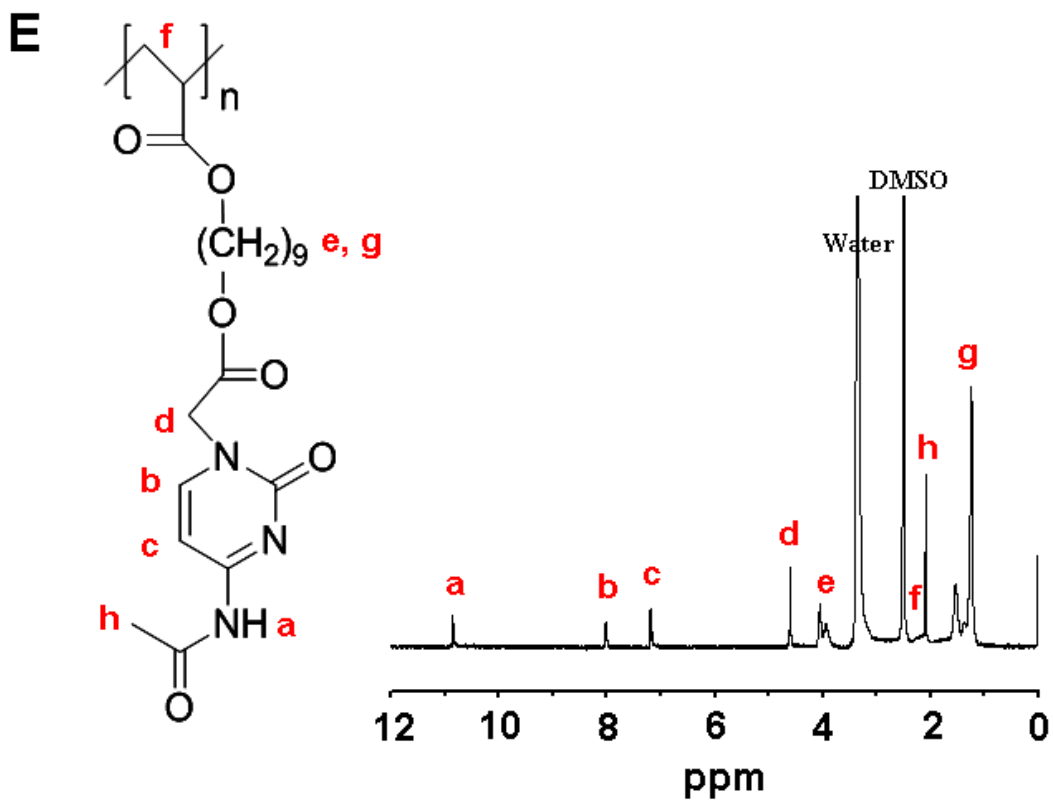

Fig. S31 ^{1}H NMR spectra of DNA-mimicking brush polymers measured in DMSO-d_6: (A) P9HNA-A; (B) P9HNA-G; (C) P9HNA-T; (D) P9HNA-U; (E) P9HNA-C.

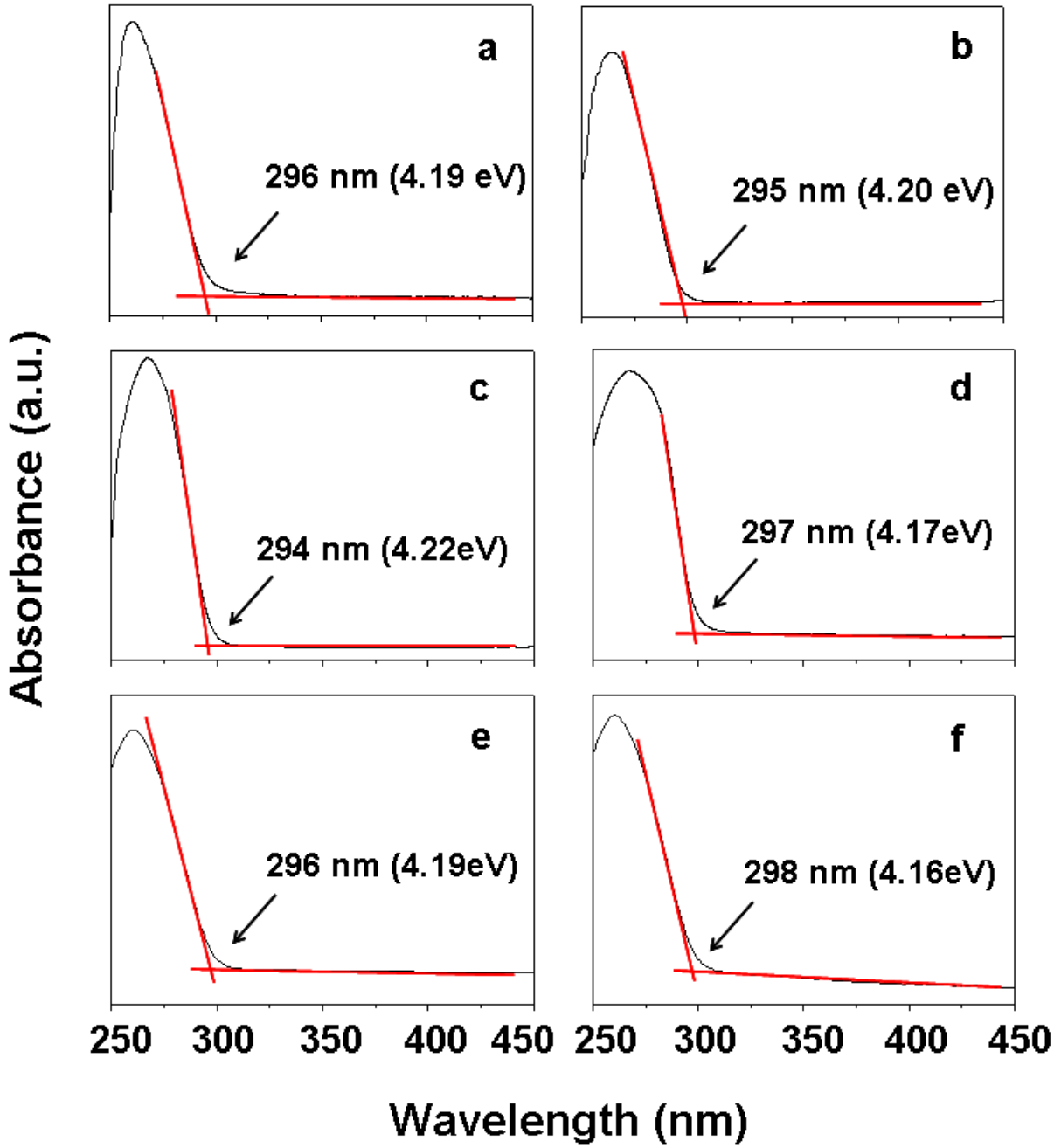

Fig. S32 UV-vis spectra of DNAs coated on quartz substrates: (a) StDNA (natural form); (b) CtDNA (natural form); (c) StDNA (salt form); (d) CtDNA (salt form); (e) StDNA (surfactant complex); (f) CtDNA (surfactant complex).

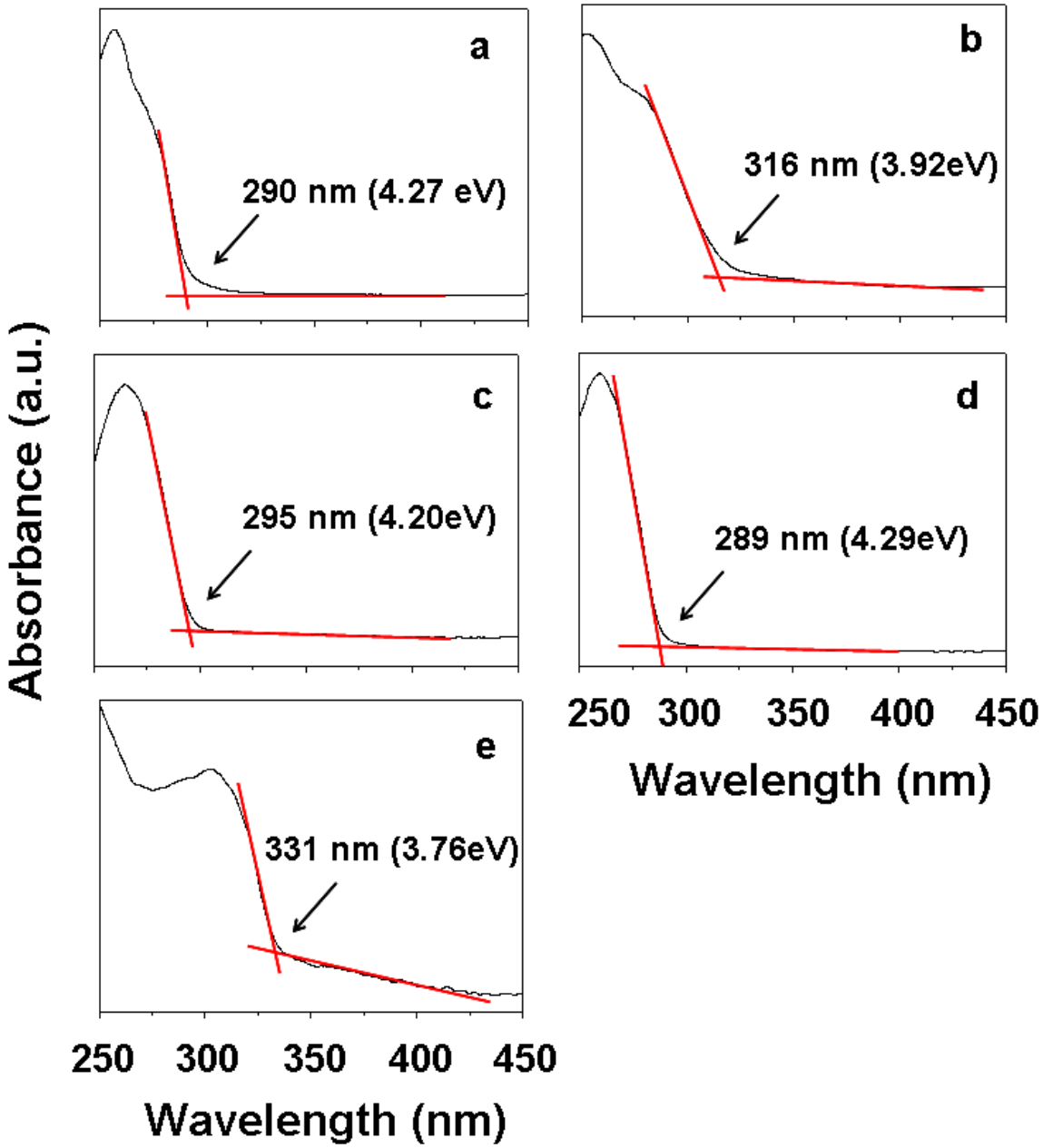

Fig. S33 UV-vis spectra of DNA-mimicking brush P4HBA polymers coated on quartz substrates: (a) P4HBA-A; (b) P4HBA-G; (c) P4HBA-T; (d) P4HBA-U; (e) P4HBA-C.

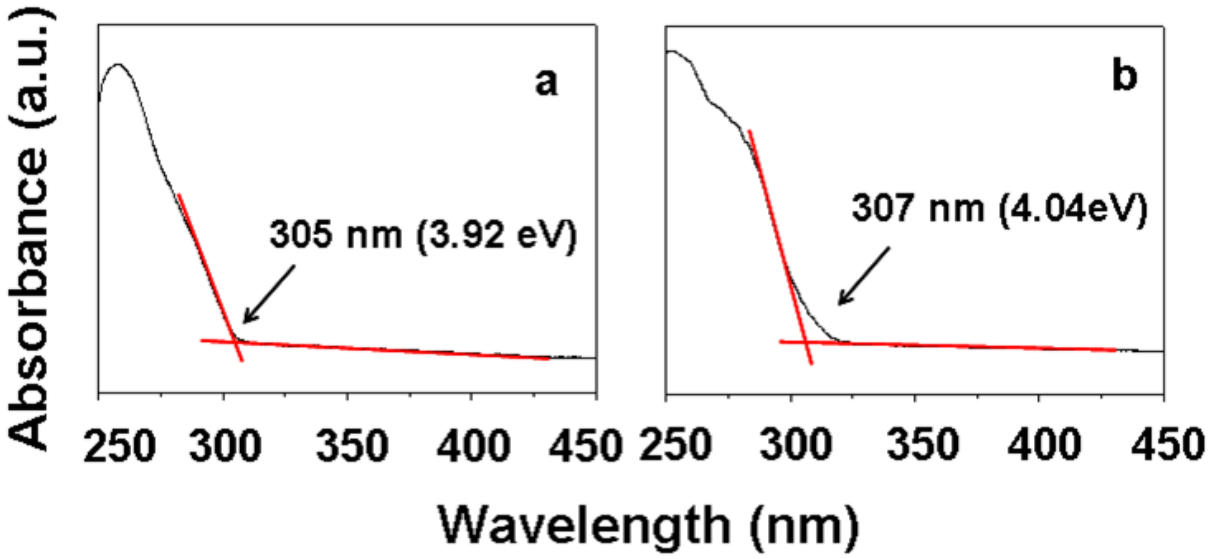

Fig. S34 UV-vis spectra of DNA-mimicking brush P9HNA polymers coated on quartz substrates: (a) P9HNA-A; (b) P9HNA-G.

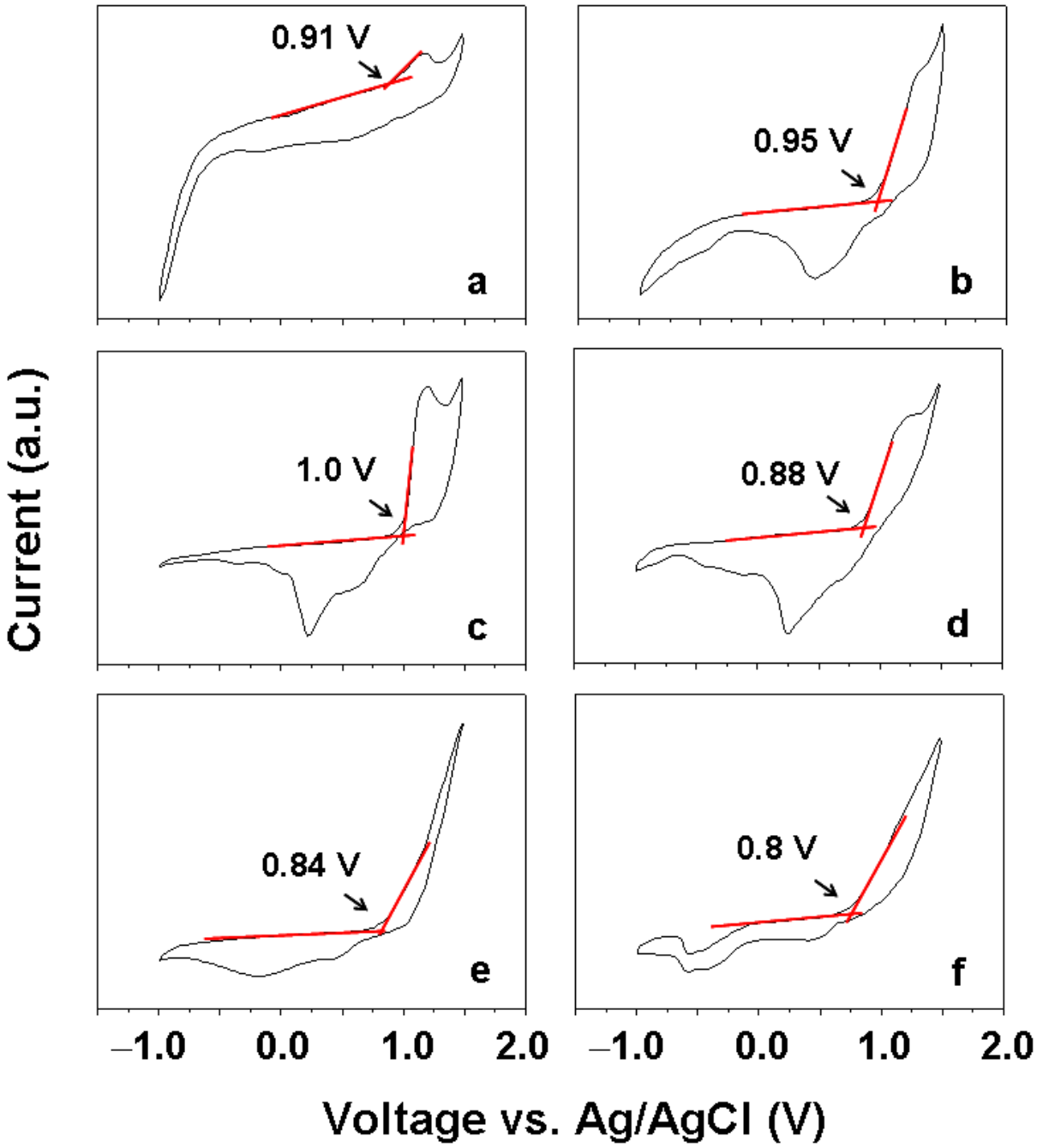

Fig. S35 CV responses of DNAs, which were fabricated with Au electrodes supported by silicon substrates: (a) StDNA (natural form); (b) CtDNA (natural form); (c) StDNA (salt form); (d) CtDNA (salt form); (e) StDNA (surfactant complex); (f) CtDNA (surfactant complex).

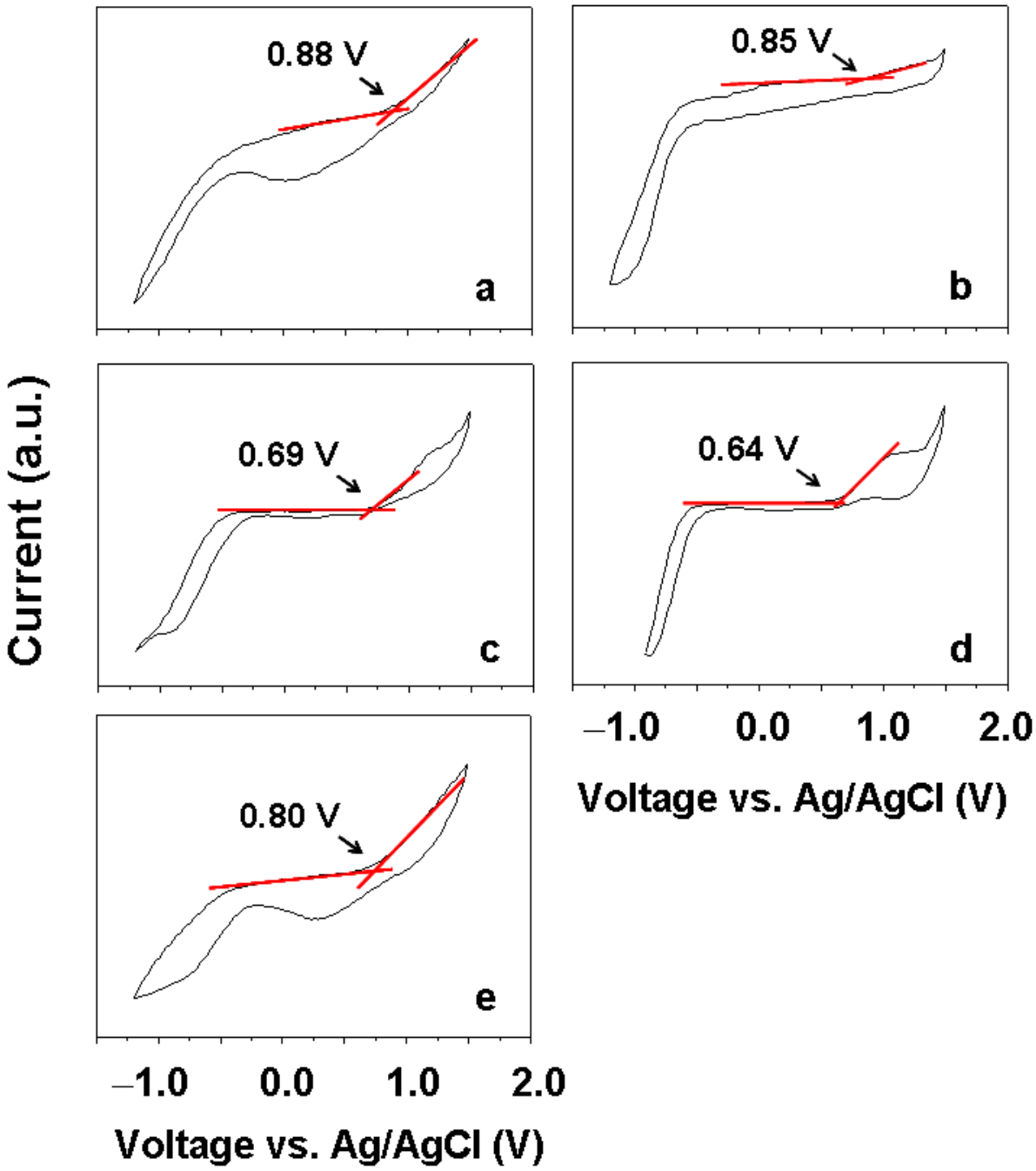

Fig. S36 CV responses of DNA-mimicking brush P4HBA polymers, which were fabricated with Au electrodes supported by silicon substrates: (a) P4HBA-A; (b) P4HBA-G; (c) P4HBA-T; (d) P4HBA-U; (e) P4HBA-C.

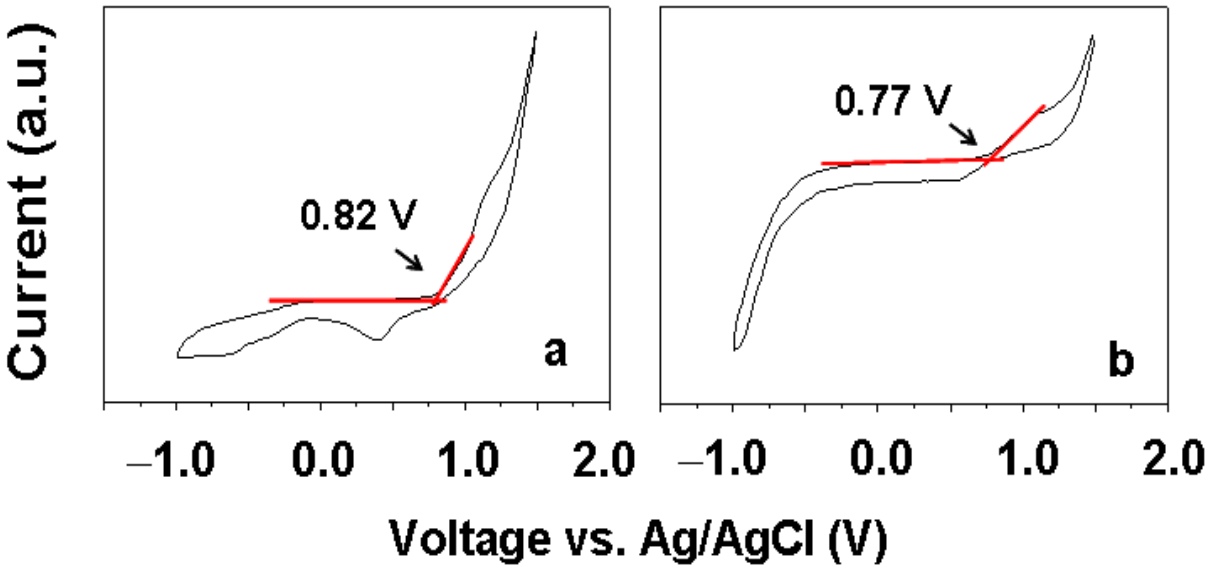

Fig. S37 CV responses of DNA-mimicking brush P9HNBA polymers, which were fabricated with Au electrodes supported by silicon substrates: (a) P9HNA-A; (b) P9HNA-G.